BTA/PE/11-14

Influence of Chemical reactions on In Situ Combustion: a Simulation Study

19 July, 2011

Ahmed Hussain

Department of Geotechnology

Delft University of Technology

Title	:	Influence of chemical reactions on In Situ Combustion: a simulation study

Author(s)	:	Ahmed Hussain
Date	:	July 2011
Professor(s)	:	dr. ir. E.S.J Rudolph
Supervisor(s)	:	Negar Khoshnevis Gargar MSc
TA Report number	:	BTA/PE/11-14
Postal Address	:	Section for Petroleum Engineering Department of Applied Earth Sciences Delft University of Technology P.O. Box 5028 The Netherlands
Telephone	:	(31) 15 2781328 (secretary)
Telefax	:	(31) 15 2781189

Abstract

In-situ combustion (ISC) is an enhanced oil recovery process during which air or oxygen-enriched air is injected into a reservoir. The oil in the reservoir reacts with the oxygen and the so-called combustion front is formed and propagates through the reservoir, generating heat and flue gases. During the process, numerous chemical reactions take place in different zones and temperature ranges. For the description of the process the oil is represented by pseudo components. The definition of the pseudo component defines the reaction schemes implemented in the numerical simulator. The reaction kinetics are described by relative simple order reactions for which the reaction rates are calculated using the Arrhenius-type equations. Estimating the input parameters of the Arrhenius equation is a giant obstacle in ISC modelling. Combustion tube experiments are performed to acquire oil, water and gas production data, the effluent composition and temperature profiles which depend on the oil and reservoir rock properties. Estimating the Arrhenius parameters can be done by history matching these experiments. Due to the quite large amount of parameters non-unique solutions are found. Unfortunately, so far the resulting adjusted parameters are not tested if they describe a chemical-physical sound and realistic behavior.

In this research an ISC tube experiment with an Athabasca bitumen was simulated using a commercial thermal simulator (CMG STARS). The cumulative oil and gas production and the temperature profiles of the experiment were used for verification of the simulations. The first simulation was done with the input parameters as stated by Yang and Gates (2009). In this simulation the reaction rate parameters were chosen such that coke formation from asphaltene by cracking already commences at temperatures of around 343 K and coke formation from asphaltenes by oxidation at temperatures of around 650 K. Further, in the applied reaction schemes methane combustion is assumed to be up to a factor 10^{30} slower than hydrocarbon gas combustion.

In this study, the reaction kinetics were changed to see the influence of the reaction kinetics parameters of asphaltene cracking and asphaltene oxidation at lower temperatures. Further, the reaction rates describing methane combustion was set equal to the kinetic parameters of hydrocarbon gas combustion. From these simulations it was found that the hydrocarbon gas combustion reaction does not significantly influence the ISC process. Changing the reaction kinetics of asphaltene cracking and oxidation does influence the ISC process significantly; asphaltene cracking occurs fasters and starts at lower temperature, more coke is formed and combusted in the simulation but less oil is produced than in the base case.

Furthermore, the injection rate of the air was varied to identify the impact of the fuel/oxygen ratio on the production data. A higher air injection rate shows that the combustion front moves through the reservoir in a shorter amount of time; which indicates that it is possibly economically favorable to inject air at a higher rate into an oil reservoir in which ISC is conducted.

Table of Contents

List of symbols

A:	frequency factor	[ ]
E_a:	activation energy	$[\frac{J}{mole}]$
T:	temperature	$[K]$
P:	pressure	$[Pa]$
R:	universal gas constant	$[\frac{J}{mole\ K}]$
k:	reaction rate	$[\frac{mole}{s}]$
V_{isg}:	gas viscosity of component i	$[Pa\ s]$
V_g:	combined gas viscosity of all component i	$[Pa\ s]$
$A_{vg}\{i\}$:	First coefficient in correlation for temperature dependence of viscosity of component i in the gas phase.	$[Pa\ s]$
$B_{vg}\{i\}$:	second coefficient in correlation for temperature dependence of viscosity of component i in the gas phase.	$[Pa\ s]$
$\mu_{asphaltene}$:	viscosity of asphaltene	$[Pa\ s]$
$\mu_{maltene}$:	viscosity of maltene	$[Pa\ s]$
y{i}:	mole fraction of gas component i	[ ]
HTO:	high temperature oxidation	[ ]
LTO:	low temperature oxidation	[ ]

List of Figures

List of Tables

Introduction

New discoveries of conventional giant oil reservoirs like the Ghuwair field in Saudi Arabia, the Spindletop field in Texas, USA or the Midway-Sunset field in California, USA are becoming rarer[1]. Most of the giant oil reservoirs are (close to) depleted, yet the world is still craving for cheap oil. Oil sands represent a large portion of hydrocarbon deposits in the world. Cyclic Steam Simulation (CSS) is the most widely used technique for exploiting these deposits. With CSS a recovery of 15 to 20% of the oil-in-place is possible, a follow-up process is required to improve recovery[2].
For heavy oil fields, In-Situ Combustion (ISC) is seen as a recovery process with much potential. Experiments indicate that recovery levels of 60-70% pore volume might be reached. Unfortunately ISC is not well understood and controlling the process in pilot fields is[3].

In Situ Combustion (ISC) is a complex oil recovery process in which thermal energy is generated inside the reservoir by combustion reactions of the oil and injected air. Chemical reactions take place in different transient zones and over a wide temperature range. These chemical reactions are numerous and generally divided into three main groups in ascending temperature ranges[4]. Low Temperature Oxidation (LTO) reactions are combustion reactions in which oxygen reacts with the oil to form partially oxidized products (temperatures below 350 °C). At intermediate temperatures, fuel (coke) is formed by cracking of the crude oil (temperatures between 350 and 400 °C). High Temperature Oxidation (HTO) reactions are combustion reactions in which the fuel, the formed coke, reacts with oxygen forming carbon oxides and water (temperatures above 400 °C)[6].

During ISC water and light oil in the reservoir evaporate and move away from the combustion front, sweeping with them liquid oil, water and gas (see Figure 2.1). The mobilized light oil mixes with the native oil reducing the viscosity of the oil. Further away from the combustion front, the water condensates because the temperature drops and a hot water bank is formed. The leading edge of this bank is the primary area where the oil is banked by the hot water. These driving mechanisms are not investigated in this research, only the chemical reactions are concentrated upon.

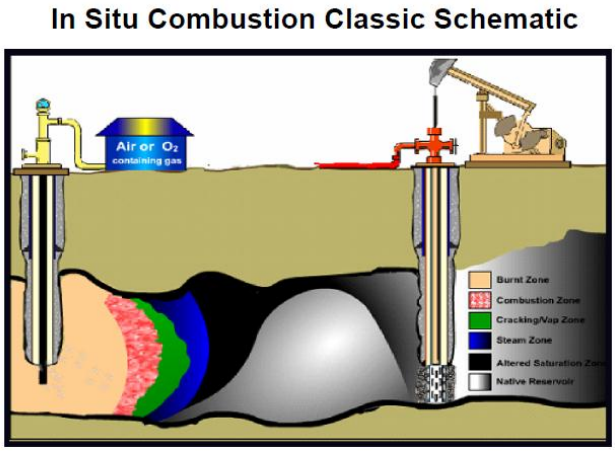

Figure 1. 1: Schematic In Situ Combustion process (Not to scale) (Szeoke (2007))

One of the challenges applying ISC as an EOR method is to control the process. In particular, the injection of the right amount of air and the prediction of air break-through are challenges. By numerical simulation, the oil recovery can be estimated for different production scenarios. These simulations are useful for optimising production methods and for designing laboratory experiments. It is of great importance that the model used for the simulations represents the main physical and chemical mechanisms of the in-situ combustion process correctly.

Yang & Gates (2009) performed simulations using the commercial simulator CMG STARS for the description of the combustion tube experiments of Belgrave et al (1990). They used the cumulative production of oil and gas and the temperature profiles to adjust the kinetic parameters of the various incorporated chemical reactions. However, they have not tested the quality of the obtained kinetic parameters.

The chemical reactions that take place have a strong influence on the ISC process and thus also on the prediction of the amount of air injected or the air break-through. The reaction scheme depends on the chosen characterization of the oil. As the oil is commonly described by pseudo-components, the input parameters of the reactions are commonly not known and, therefore, are fitted to the production and temperature profile of combustion tube experiments. Due to the rather large amount of parameters describing only the chemical reactions non-unique solutions are found. Unfortunately, the resulting adjusted parameters are not tested if they describe a chemical-physical sound and realistic behavior. Additionally, in literature there is still some discussion about the reaction schemes and their importance. For example, according to Marin (2007) LTO reactions are crucial to be incorporated. This has also been shown by experiments[6]. Still in other work LTO reactions are completely ignored[5].

Therefore finding the best representation (with respect to its chemical-physical behaviour and numerical simplicity) of the ISC processes from the different published models is quite a task. Analysing the published models and then correcting them will eventually lead to a plausible representation of the ISC processes.

The objective of this research is to investigate the importance of gas phase combustion and of the cracking reaction for the overall description of ISC. For this purpose the kinetic parameters describing these chemical reactions were varied. For the simulations the model as suggested by Belgrave et al. (1990) and of Yang and Gates (2009) has been used as a base model. The oil is characterized in terms of maltenes and asphaltenes which results in products such as asphaltenes, coke, carbon di- and monoxides, water and hydrocarbon gases. By varying the kinetic parameters and analyzing the saturations of the various components per grid block it could be identified which kinetic parameters give realistic description of the process and which chemical reactions are crucial to be incorporated.

In chapter 2 the theory of in-situ combustion is covered. The characterisation of the oil and its properties, the various chemical reactions and reaction schemes, the reaction rates and a general description of combustion tube experiments are treated.

In chapter 3 the details of the numerical simulation model are given. This includes an introduction to CMG STARS and the description of the model set-up. The rock fluid properties and input parameters used for the simulation are given here.

In chapter 4 the results of the simulations are presented and discussed.

Chapter 5 reports the conclusions of this work.

Theory

Characterization of the oil and its properties

Oil consists of a huge number of different hydrocarbons and other molecules. On average they consist of 85% carbon, 13% hydrogen and 2% nitrogen, sulfur and oxygen (in weight percentage) (Gluyas & Swarbrick (2004)).

Because the composition of crude oil is so complex, a detailed representation of a crude oil in a simulator is not possible. Therefore, commonly the composition of a crude oil is defined in terms of pseudo-components. These pseudo components are combinations of various hydrocarbon types. In this work the oil is described by two pseudo-components, namely asphaltenes and maltenes, as suggested by Yang & Gates (2009). In figure 2.1 the characterization according to the so-called SARA model is shown. It can be seen that the description of the oil by maltene and asphaltene is a simplification of the SARA model.

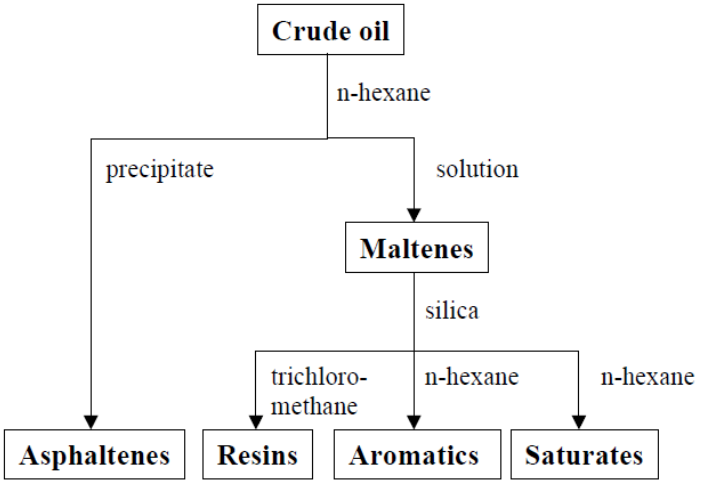

Figure 2. 2: SARA–Separation scheme (*Strausz, O.P. and E.M. Lown* (2003))

The definitions of the SARA model will be given to clarify the model used in this research.

Saturates: Saturates are saturated non-polar hydrocarbons, i.e. alkanes and cycloalkanes (naphtenes). The amount of saturates in a crude oil decreases with an increasing specific weight of the oil. Often saturates form the lightest fraction of the crude oil[7].

Aromatics: Aromatics refer to benzene and its structural derivatives. Aromatics are the smallest fraction in most oils (Gluyas & Swarbrick (2004). The majority of the aromatics contain alkyl chains and cycloalkane rings along with additional aromatics rings. Aromatics are often classified as mono-, di-, tri-aromatics depending on the

number of aromatics rings present in the molecule. Polar, higher weight aromatics may fall in the resin or asphaltene fraction[8].

Resins: This fraction consists of polar hydrocarbon molecules often containing heteroatoms such as nitrogen, oxygen, or sulfur. A common definition of resins is the fraction of the oil which is not a saturate or an aromatic but soluble in n-hexane. Resins are soluble in light alkanes such as pentane and heptanes but insoluble in liquid propane. Resins are structurally similar to asphaltenes but have a higher H/C ratio, and lower molecular weight (1000g/mole)[4].

Asphaltenes: This fraction is defined as the fraction which is not soluble in n-hexane. The precipitate is soluble in aromatic solvents like toluene and benzene. Asphaltenes are similar to resins but have a higher molecular weight, typically 500-1500 g/mole. The asphaltene fraction contains the largest percentage of heteroatoms (O, S, and N) and organometallic constituents (Ni, V, Fe) in the crude oil. The structure of asphaltene molecules is believed to consist of polycyclic clusters substituted with varying alkyl side chains (Aske et al. (2002)).
For the characterization of the oil in terms of maltenes and asphaltenes the saturated, the aromatics and the resins are combined to one pseudo component. The asphaltenes are considered separately because the content of these components give the specific behavior of heavy oils[4]. In table 2.1 the initial oil composition as used for the simulations in this work is given.

	Fraction	Specific weight
Maltenes	0.915	407 (g/mole)
Asphaltenes	0.085	1090 (g/mole)

Table 2. 1: Initial oil composition and molecular weights of the pseudo-components (Yang & Gates (2009))

Reaction kinetics

The reaction kinetics describe how fast a chemical reaction occurs and how much of the reactant is used to produce a certain amount of product. Reaction kinetics are important for the understanding of in-situ combustion for the following reasons:

- Characterization of oil reactivity.
- Identifying at which conditions ignition will occur.
- Characterization of possible fuel formation by chemical reactions and its impact on combustion.
- To acquire input parameters (e.g. reaction rate model) for the numerical simulation of ISC processes.

Combustion of crude oil in porous media is a complex system of reactions; reactions compete and their reaction rates are temperature dependent. Because crude oils on themselves are complex, it is impossible to represent all the reactions that occur during ISC. Detailed models for hydrocarbon oxidation reactions are available only for simple hydrocarbon molecules and contain even the most detailed reactions on the level of radicals[8]. Simplified models describing the chemical reactions during in-situ combustion processes have been developed in recent years[5].

Chemical reactions

Below the reactions which are used to describe the ISC are shortly described. Some of these reactions compete for the same reactants, others build on the products of another reaction.

Thermal cracking

Under high temperatures the carbon-carbon bonds of heavier hydrocarbon components are broken into smaller hydrocarbon molecules and an immobile fraction which is called coke[8].

Low Temperature Oxidation (LTO)

At temperatures below 350 °C, LTO reactions predominate, which involve the addition of oxygen to the maltenes and ashpaltenes producing heavier oxidized compounds[4]. The transition between the LTO and HTO temperature ranges is characterized by the negative temperature gradient region (NTGR) in which the global oxygen-uptake rates decrease with increasing temperature[6].

High Temperature Oxidation (HTO)

The oxidation reactions which occur at a temperature above 350 °C are defined as HTO reactions[6]. In the model used by Belgrave et al. (1990), HTO reactions oxidize (combust) the coke forming CO and CO_2.

Chemical reaction scheme

Belgrave et al. (1990) described ISC with an Athabasca bitumen. The bitumen was described in terms of maltenes and asphaltenes. Products of the various reactions are coke, methane, inert gas and hydrocarbon gas. The ISC is described by the following scheme[5].

The cracking reactions (first order):

$$Maltenes \rightarrow 0.372\ Asphaltenes \quad (2\text{-}1)$$

$$Asphaltenes \rightarrow 83.223\ Coke \quad (2\text{-}2)$$

$$Asphaltenes \rightarrow 37.683\ Hydrocarbon\ Gas \quad (2\text{-}3)$$

The LTO reactions (first order with respect to hydrocarbon mass fraction, 0.4246 and 4.7627 orders with respect to oxygen partial pressure for reactions (2-4) and (2-5), respectively)

$$Maltenes + 3.431\ O_2 \rightarrow 0.4726\ Asphaltenes \quad (2\text{-}4)$$

$$Asphaltenes + 7.513\ O_2 \rightarrow 101.539\ Coke \quad (2\text{-}5)$$

HTO or coke combustion (first order with respect to both reactants):

$$(Coke)CH_{1.13} + 1.232\ O_2 \rightarrow CO_x + 0.565\ H_2O \quad (2\text{-}6)$$

wherein CO_x is described by the $\frac{CO_2}{CO}$ molar ratio which is set equal to 8.96.

$$Methane + 2O_2 \rightarrow CO_2 + 2H_2O \quad (2\text{-}7)$$

$$HC\ Gas + O_2 \rightarrow 0.9695\ CO + CO_2 + 2H_2O \quad (2\text{-}8)$$

Chemical reaction rates

In this work the chemical reaction rates are described by Arrhenius-type equations accounting for the activation energy and frequency factor:

$$k = A * exp\left(-\frac{E_a}{RT}\right) \quad (2\text{-}9)$$

$$k = rate\ constant\ \left[\frac{mole}{s}\right]$$

$$A = frequency\ factor\ [unit\ depends\ on\ reaction\ order]$$

$$E_a = activation\ energy\ \left[\frac{J}{mole}\right]$$

$$T = temperature\ in\ [K]$$

$$R = gas\ constant\ 8.314\left[\frac{J}{mole\ K}\right]$$

The determination of the parameters describing the kinetics of the different chemical reactions is challenging due to the large number resulting in solutions which are non-unique. Unfortunately, it seems that, e.g., in the paper of Yang and Gates the resulting adjusted parameters have not been tested if they describe a chemical-physical sound and realistic behavior.

General description of In-Situ Combustion and of combustion tube experiments

Yang and Gates used combustion tube experiments to adjust kinetic parameters and/or to verify the simulation results[5]. These combustion tube experiments were done in Calgary in the group of Belgrave[5]. Here the combustion experiment is shortly explained to allow comparison of the simulation results with the experimental results.

A packed bed of sand saturated with oil and, in the case of wet ISC, water is placed in a tube. The experiment is set up as a one dimensional, vertical test. Air is injected at the top end of the tube, oil, water and gases are produced at the lower end. The experiment is done adiabatically. This has been established by insulating the tube and heating it from the outside to compensate for possible heat losses towards the surroundings. After air injection, the oil ignites and is partially combusted. The combustion front then moves through the combustion tube in direction of the producing end. During the experiment the temperature and pressure are monitored at different vertical positions. After the experiment, the coke deposition in the sand is examined[5].

The combustion tube experiments were performed at various conditions. The reservoir temperature is 90 °C, the injection temperature is 400 °C and the air injection rate is 1.344 m^3/day. The temperature in the tube combustion experiment reaches a maximum temperature of about 800 °C and the pressure reaches a maximum of 2 atm[5].

Numerical simulation model

Introduction to CMG STARS

The commercial simulator CMG STARS, the Steam Thermal Advanced Reservoir Simulator, was developed by the Computer Modeling Group in Calgary. STARS is a comprehensive numerical simulation tool which can be used to model compositional, steam, geomechanical (fracturing, compaction, rock failure), dispersed component (polymers, gels, fines, emulsions, foams), and in-situ combustion processes[10]. With the help of CMG Stars processes on field scale, pilots and laboratory scale can be simulated.

Reservoir and process description

The total length of the one-dimensional reservoir used for the simulations is 1.83 m. The reservoir is split up into 200 grid blocks with dimensions 0.0881m(w)x0.0881m(d)x0.00915m(h) (see Figure 3.1). Air or air enriched with oxygen is injected from the top; oil is produced from the bottom of the tube at grid block (1,1,200). In table 3.1 the composition of the injected air as function of time is given. The oxygen content in the air is gradually increased from 0% to 95% of the volume. At all times the injection rate is 1.334 m^3/day; in the first 7 hours the injection temperature is 400 °C. After 7 hours the injected air is only heated up to 100 ° C, the reservoir temperature. After ignition was established the combustion propagates in vertical direction downwards towards the producer. The initial conditions of the combustion tube are the same as given by Belgrave et al. (1990) and are 4100 kPa and 90°C.

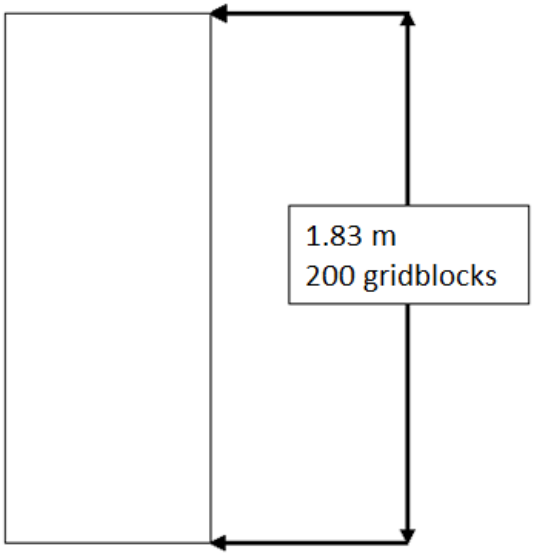

Figure 3. 1: Schematic drawing of the combustion tube experiment

	Air composition			
Time (hr)	O_2	N_2	Temperature (°C)	Flow rate (m^3/day)
0.00	0%	100%	400	1.334
0.12	17%	83%	400	1.334
0.24	40%	60%	400	1.334
0.40	54%	46%	400	1.334
0.50	70%	30%	400	1.334
7.00	95%	5%	400	1.334
6.42	95%	5%	250	1.334
7.92	95%	5%	180	1.334
16.47	95%	5%	100	1.334

Table 3. 1: Composition and temperature of the injected air (Yang & Gates (2009))

Main base case description

In the combustion experiments of Yang & Gates (2006) and Belgrave et al. (1990) Athabasca bitumen was used. Extensive research has been conducted on this kind of heavy oil. Yang & Gates fitted the input parameters describing the kinetics to the production curves of the oil, gas and liquid components (see figure 3.2). The input parameters of Yang and Gates (2006) are used for the base case simulations of this research.

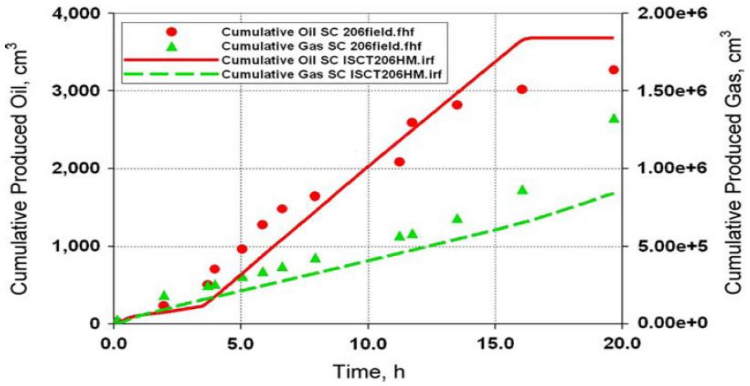

Figure 3. 2: Cumulative oil and gas production from experiment Test 206 (data points) by Belgrave et al. (1990) and history-matched simulation results (lines) (Yang & Gates (2009)).

Assumptions and general descriptions (Base case)

The characterization of the oil according to Belgrave et al. (1990) is used in this research. This means the oil consists of maltene and asphaltene. The Yang & Gates (2009) reaction scheme (see table 3.2) is implemented. The incorporated reactions produce water, hydrocarbon gas, carbon mono- and dioxide, and coke. The chemical reaction rates are calculated by Arrhenius-type equations (see chapter 2) of which the input parameters are given in table 3.3. The components occur in four phases: liquid oil phase, liquid aqueous phase, gas phase and solid phase (see table 3.4). The reservoir, the overburden and the underburden layers have the same initial temperature. No heat losses are taken into account in vertical direction. The horizontal heat loss parameters are given in table 3.5.

1.	$Maltenes \rightarrow 0.372\ Asphaltenes$	(2-1)
2.	$Asphaltenes \rightarrow 83.223\ Coke$	(2-2)
3.	$Asphaltenes \rightarrow 37.683\ Hydrocarbon\ Gas$	(2-3)
4.	$Maltenes + 3.431\ O_2 \rightarrow 0.4726\ Asphaltenes$	(2-4)
5.	$Asphaltenes + 7.513\ O_2 \rightarrow 101.539\ Coke$	(2-5)
6.	$(Coke)CH_{1.13} + 1.232\ O_2 \rightarrow CO_x + 0.565\ H_2O$	(2-6)
7.	$Methane + 2O_2 \rightarrow CO_2 + 2H_2O$	(2-7)
8.	$HC\ Gas + O_2 \rightarrow 0.9695\ CO + CO_2 + 2H_2O$	(2-8)

Table 3. 2: The reaction scheme which is implemented in the simulation model

Reaction	A	E_a	H_r
	Frequency factor	Activation Energy	Heat of reaction
		(J/mol)	(J/mol)
1	4.05×10^{10} day^{-1}	1.16×10^{6}	0
2	1.82×10^{4} day^{-1}	4.02×10^{4}	0
3	1.18×10^{14} day^{-1}	1.76×10^{5}	0
4	2.12×10^{5} day^{-1} $kPa^{-0.4246}$	4.61×10^{4}	1.30×10^{6}
5	1.09×10^{5} day^{-1} $kPa^{-4.7627}$	3.31×10^{4}	2.86×10^{6}
6	3.88×10^{0} day^{-1} kPa^{-1}	8.21×10^{2}	4.95×10^{5}
7	3.02×10^{10} day^{-1} kPa^{-1}	5.95×10^{4}	8.91×10^{5}
8	1.31×10^{8} day^{-1} kPa^{-1}	2.66×10^{5}	4.44×10^{5}

Table 3. 3: Base case reaction kinetics (Yang & Gates (2009))

Components	Oil	Gas	Aqueous	Solid
Water			X	
Maltenes	X	X		
Asphaltenes	X			
Oxygen		X		
Nitrogen		X		
Hydrocarbon gas	X			
Carbon monoxide	X			
Carbon dioxide	X			
Methane	X	X		
Coke				X

Table 3. 4: Base case phase distribution of components (Yang & Gates (2009))

Heat Capacity (J/m^3 °C)	6.20E+04
Thermal Conductivity (J/m day °C)	6.50E+04

Table 3. 5: Heat loss parameters in horizontal directions (Yang & Gates (2009))

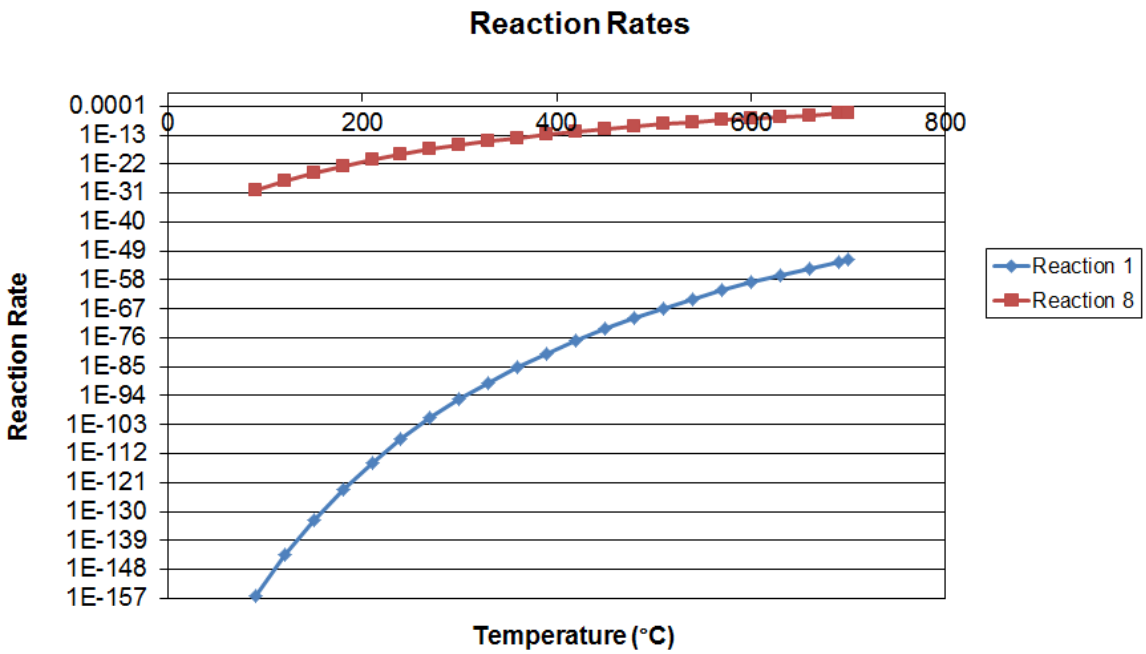

Figure 3. 3: Reaction rates as function of temperature for reaction 1 and reaction 8 as used for the base case (see table 3.3).

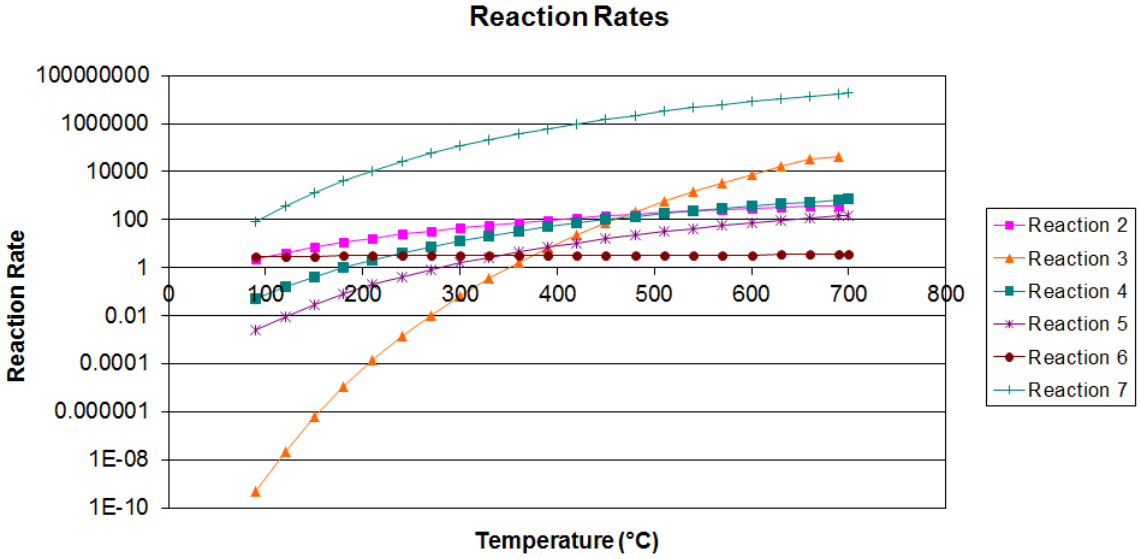

Figure 3. 4: Reaction rates as function of temperature for reaction 2 to reaction 7 as used in the base case simulation (see table 3.3).

Relative permeability

The normalized Stone's model (Yang & Gates (2009)) was used to describe the three-flow phase flow assuming that water is the wetting phase, gas the non-wetting phase and oil is the intermediate-wetting phase[5]. The simulator uses two-phase relative permeability parameters to generate three-phase relative permeability data. The phase imbibition and drainage curves used in this work are based on the paper of Belgrave et al. (1990) and are given in table 3.6. Since in ISC the temperature in the reservoir changes over time and position, the temperature dependence of the relative permeability needs to be taken into account. Table 3.7 details the endpoint relative permeability for two different temperatures, namely 15 °C and 800 °C

	Oil/Water			Gas/Oil	
S_w	K_{rw}	K_{row}	$S_o + S_w(S_l)$	K_{rg}	K_{rog}
0.05000	0.00000	1.00000	0.07000	0.10000	0.00000
0.10000	0.00039	0.88581	0.16000	0.08615	0.00316
0.15000	0.00156	0.77855	0.21000	0.06632	0.01262
0.25000	0.00625	0.58478	0.31000	0.03711	0.05050
0.35000	0.01406	0.41869	0.41000	0.01881	0.11362
0.45000	0.02500	0.28028	0.51000	0.00829	0.20199
0.65000	0.03906	0.08651	0.61000	0.00296	0.31562
0.75000	0.05625	0.03114	0.71000	0.00073	0.45449
0.85000	0.07656	0.00346	0.80000	0.00011	0.60106
0.95000	0.10000	0.00000	0.95000	0.00000	0.89080
1.00000	0.12656	0.00000	1.00000	0.00000	1.00000

Table 3. 6: Relative permeability data (Belgrave et al. 1990)

Relative Permeability Curve Endpoints	15°C	800°C
S_{wirr}	0.05	0.00679
S_{orw}	0.15	0.295
S_{org}	0.05	0.350
S_{gc}	0.07	0.0266
K_{rwro}	0.10	0.0508
K_{rocw}	1.00	0.503

Table 3. 7: Temperature dependence of endpoint relative permeability (Yang & Gates (2009))

Liquid Viscosities

The description of the liquid phase viscosity used for the base case and the other simulations are taken from Belgrave et al. (1990).
The viscosities of bitumen, maltene and asphaltene are described by the following equations:

$$\mu_{bitumen} = 0.48267 \times 10^{-6} \exp\left(\frac{7685.2}{T}\right) \quad (3\text{-}1)$$

$$\mu_{maltene} = 0.19359 \times 10^{-4} \exp\left(\frac{5369.2}{T}\right) \quad (3\text{-}2)$$

From the viscosities of maltene and bitumen, the viscosity of asphaltene can be determined because the bitumen is described as a mixture of maltene and asphaltene:

$$\mu_{bitumen} = (\mu_{maltene})^{x_{maltene}} * (\mu_{asphaltene})^{x_{asphaltene}} \quad (3\text{-}3)$$

Resulting in the following expression:

$$\mu_{asphaltene} = 4.892 \times 10^{-25} \exp\left(\frac{33147}{T}\right) \quad (3\text{-}4)$$

Gas viscosity

The gas phase consists, among others, of light hydrocarbon components such as methane, carbon mono- and dioxide. Assuming ideal behavior the gas phase viscosity can be described by a combination of the viscosities of the gas phase components (see eq 3-5). The viscosity of each component is described by an empirical equation (eq 3-6):

$$V_g = \frac{\sum_{i=1}^{numy} V_{isg}(i) \times y(i) \times \sqrt{cmm(i)}}{\sum_{i=1}^{numy} y(i) \times \sqrt{cmm(i)}} \quad (3\text{-}5)$$

$$V_{isg} = A_{vg}(i) \times (T^{B_{vgi}}) \quad (3\text{-}6)$$

Equilibrium ratio (K-Value)

The vapor-liquid phase equilibrium, meaning the distribution of a component over the gas and the liquid phase (evaporation), is described with the so-called equilibrium constant or distribution coefficient K. The K-values can either be computed with the help of equations of state or with correlations. For this study the correlations (eq. 3-7) given below with the parameters given in table 3.8 are used.

$$\text{The Gas} - \text{Liquid K} - \text{Value Correlation} = \left(\frac{k_{v1}}{P}\right) e^{\frac{k_{v4}}{T - k_{v5}}} \quad (3\text{-}7)$$

Component	K_{v1}	K_{v4}	K_{v5}
Maltenes	1.89×10^{7}	-6560	-80.1
Asphaltenes	0	0	0
Water	1.18×10^{7}	-3820	-227
Hydrocarbon Gas	8.62×10^{8}	-3100	-273
CH4	5.45×10^{5}	-879	-266
CO2	8.62×10^{8}	-3100	-273
CO	2.32×10^{5}	-530	-260

Table 3. 8: Component specific parameters for the computation of K-values using eq. 3-7 (CMG, 2007)

Heat exchange between the different phases

For the description of how the heat is captured in certain components, the specific heat capacities of the components forming the different phases were used. To describe the temperature dependence of the heat capacities correlations are used. The temperature dependence of gas phase heat capacities is much stronger than the temperature dependence of the liquid phase. Equation 3-8 gives the correlation for the description of the gas phase heat capacities, in table 3.9 the component specific parameters are given. For the computation of the heat capacities of the liquid phase equation 3-9 and the parameters given in table 3.10 are used.

Component	C_{pg1}	C_{pg2}	C_{pg3}	C_{pg4}
Maltenes	0	0	0	0
Asphaltenes	0	0	0	0
O2	28.1	-3.68×10^{-6}	1.75×10^{-5}	-1.06×10^{-8}
Hydrocarbon Gas	19.8	7.34×10^{-2}	-5.60×10^{-5}	1.71×10^{-8}
CH4	19.3	5.21×10^{-2}	1.20×10^{-5}	-1.13×10^{-8}
CO2	19.8	7.34×10^{-2}	5.60×10^{-5}	1.71×10^{-8}
CO	30.9	-1.29×10^{-2}	2.79×10^{-5}	-1.27×10^{-8}
N2	31.2	-1.36×10^{-2}	2.68×10^{-5}	-1.17×10^{-8}

Table 3. 9: Parameters for the computation of specific gas-phase heat capacity with equation 3-7 (CMG, 2007)

Gas heat capacity correlations:

$$C_{pg}\left(\frac{J}{gmol°C}\right) = C_{pg1} + C_{pg2}T + C_{pg3}T^2 + C_{pg4}T^3 \qquad (3\text{-}8)$$

Component	C_{pl1}	C_{pl3}	C_{pl3}	C_{pl4}
Maltenes	994	0	0	0
Asphaltenes	2510	0	0	0
O2	46.4	-3.95×10^{-1}	-7.05×10^{-3}	3.99×10^{-5}
Hydrocarbon Gas	-3980	5.25×10^{-1}	-2.27×10^{-1}	3.29×10^{-4}
CH4	-0.02	1.20	-9.87×10^{-3}	3.17×10^{-5}
CO2	-3890	5.25×10^{1}	-2.27×10^{-1}	3.29×10^{-4}
CO	126	-1.70	1.70×10^{-2}	4.19×10^{-6}
N2	76.5	-3.52×10^{-1}	2.67×10^{-3}	5.01×10^{-5}

Table 3. 10: Parameters for the computation of specific gas-phase heat capacity with equation 3-7 (CMG, 2007)

Liquid heat capacity correlations:

$$C_{pg}\left(\frac{J}{gmol°C}\right) = C_{pg1} + C_{pg2}T + C_{pg3}T^2 + C_{pg4}T^3 \quad (3\text{-}9)$$

Base case input parameters

The input parameters for the base case simulation are summarized in table 3.11 to 3.13 and equations (2-1) to (2-8).

Component	Molecular Weight (g/mol)	Critical Temperature Tc °C	Critical Pressure Pc (KPa)
Maltenes	407	619	1480
Asphaltenes	1090	904	792
Coke	13.1	-	-
Water	18.0	374	22,100
O2	32.0	-119	5050
Gas	43.2	21.9	7180
CH4	16.0	-82.6	4600
CO2	44.0	31.1	7380
CO	28	-140	3490
N2	28	-147	3390

Table 3. 11: Molecular weight, critical temperature and pressure of the components included in the simulations (CMG, 2007)

Parameter	Value
Numerical grid	$1 \times 1 \times 200$
Grid size	$0.0881 \times 0.0881 \times 0.00915$
Total number of grid blocks	200
Initial water saturation	0.12
Initial oil saturation	0.70
Initial gas saturation	0.18
Initial bitumen mole fraction-Maltenes	0.915
Initial bitumen mole fraction-Asphaltenes	0.085

Table 3. 12: Simulation initial conditions incl. geometric definition of system (Yang & Gates (2009) and Belgrave et al. (1990))

Parameter	Unit	Value
Porosity		0.412
Permeability	D	11.30
Rock heat capacity	KJm^3	2280
Rock thermal conductivity	(KJmday °C)	605
Bitumen thermal conductivity	(KJmday °C)	13.40
Water thermal conductivity	(KJmday °C)	58.10
Gas thermal conductivity	(KJmday °C)	4.30
Coke density	KPa^-1	1380

Table 3. 13: Rock and oil properties (Yang & Gates (2009))

Results and discussions

Base Case

Reactions

1. $Maltenes \rightarrow 0.372\ Asphaltenes$ (2-1)
2. $Asphaltenes \rightarrow 83.223\ Coke$ (2-2)
3. $Asphaltenes \rightarrow 37.683\ Hydrocarbon\ Gas$ (2-3)
4. $Maltenes + 3.431\ O_2 \rightarrow 0.4726\ Asphaltenes$ (2-4)
5. $Asphaltenes + 7.513\ O_2 \rightarrow 101.539\ Coke$ (2-5)
6. $(Coke)CH_{1.13} + 1.232\ O_2 \rightarrow CO_x + 0.565\ H_2O$ (2-6)
7. $Methane + 2O_2 \rightarrow CO_2 + 2H_2O$ (2-7)
8. $HC\ Gas + O_2 \rightarrow 0.9695\ CO + CO_2 + 2H_2O$ (2-8)

Base Case		
Cum. Oil Production	3925	cm^3
Cum. Gas Production	817802	cm^3

Table 4.1. 1: Cumulative production of oil and gas: base case

Summary

The simulation with the parameters as given by Yang & Gates (2009) is chosen as the base case. It needs to be mentioned that in this report CO_2 and CO are split up by source, e.g. CO_2 from reaction #7 is listed as CO_2_7. In the following figures the cumulative oil and gas production, the temperature profile, pressure and coke concentration are given. Each of these figures are discussed and analyzed in the following.

Analysis

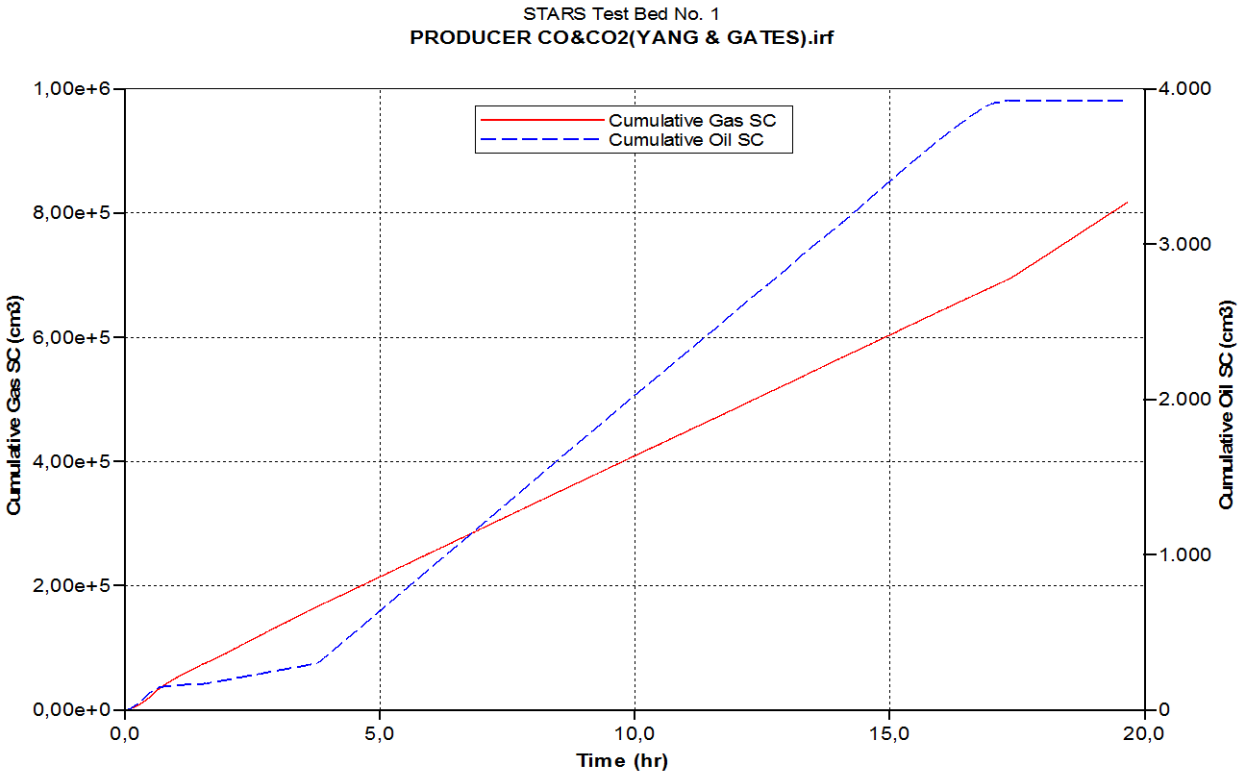

Figure 4.1. 1: Cumulative production of oil and gas at standard conditions; base case simulation.

Figure 4.1.1 shows the cumulative oil and gas production from the base case simulations. It can be seen that oil production stagnates after about 1 hour before it continuous about three hours later. The gas production increases continuously. After around 18 hours the gas production increases slightly, at the same time oil production stops.

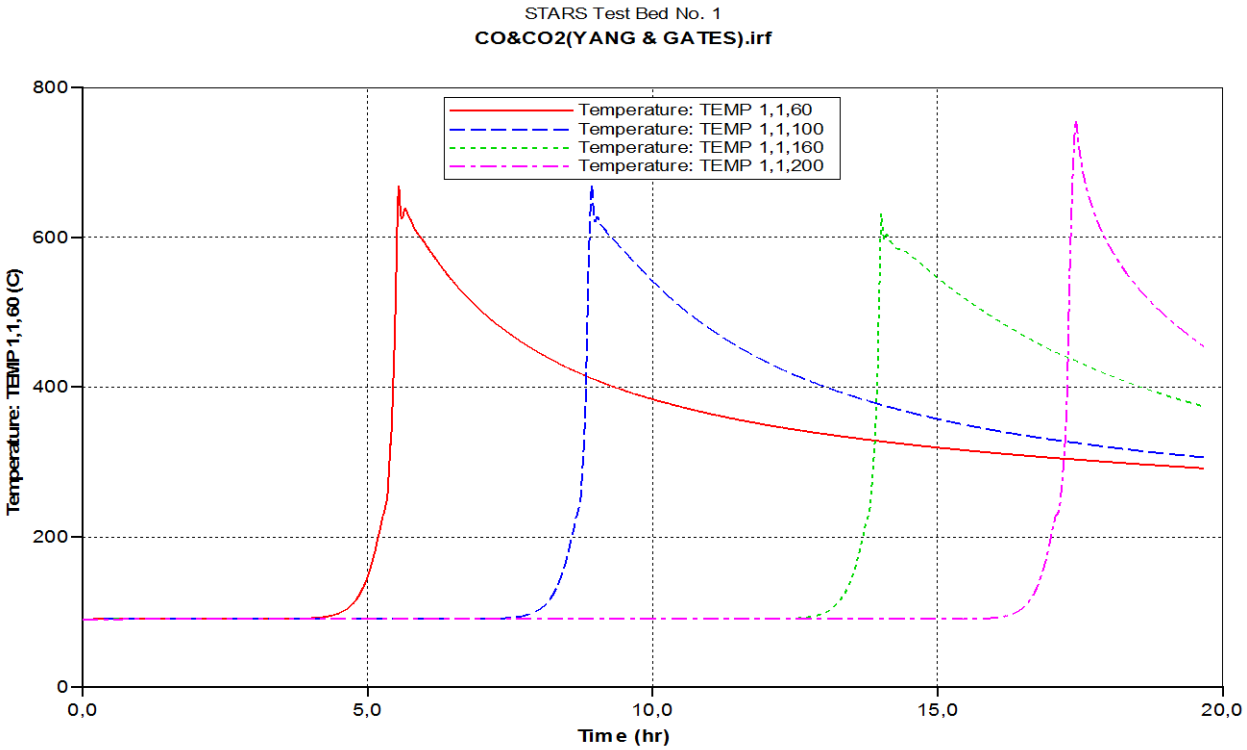

Figure 4.1. 2: Temperature profile at various positions plotted against the time; base case simulation. Position 1,1,60 is at the top close to the injector, position 1,1,200 is at the bottom of the tube at the producer.

Figure 4.1.2 shows the temperature profile at various positions. Initially the temperature in the reservoir is 90 °C. Due to coke combustion the temperature rises steeply and reaches a maximum of about 650-750 °C. Horizontal heat loss causes the temperature to decrease slowly after all the coke is combusted and oil displaced further down the combustion tube.

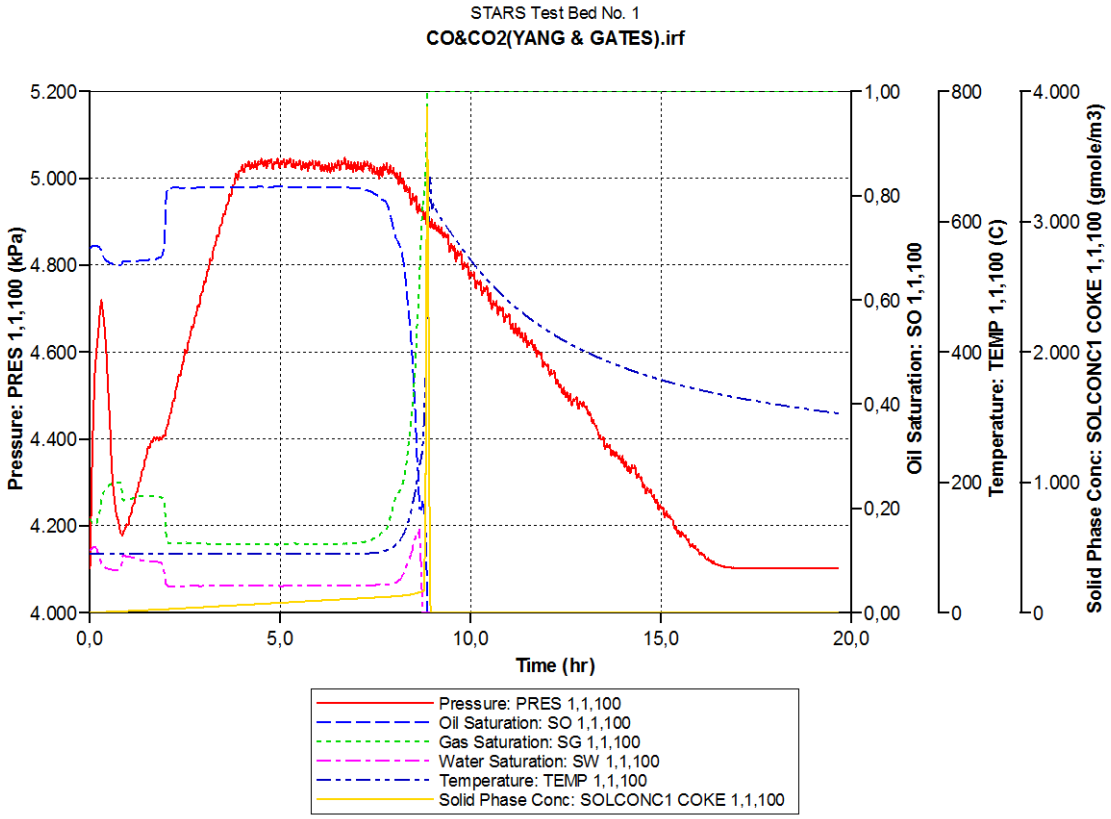

Figure 4.1. 3: Oil, gas and water saturation, temperature, coke concentration (*gmole/m³)* and pressure as function of the time in the middle of the combustion tube (1,1,100);base case simulation.

In Figure 4.1.9 the relation between the oil, gas and water saturations is shown. In the first hour the gas saturation increases because the lighter components of the oil and water evaporate (decrease of water and oil saturation). After about two hours the oil saturation rises from hydrocarbon gas condensation and due to oil banking. The oil saturation decreases steeply when coke combustion commences. It can be seen that coke formation already starts almost from the beginning. This shows that coke formation due to cracking occurs already at around 90 °C[5]. Due to the coke combustion, the temperature rises steeply. After 7.5 hours the oil saturation drops because reaction #7 and #8 start forming more coke[5] and the oil is pushed further down the reservoir due to the lower viscosity, the gas drive but also by the fire front. The water and oil saturation rise after about 8 hours, this is due to liquid banking.

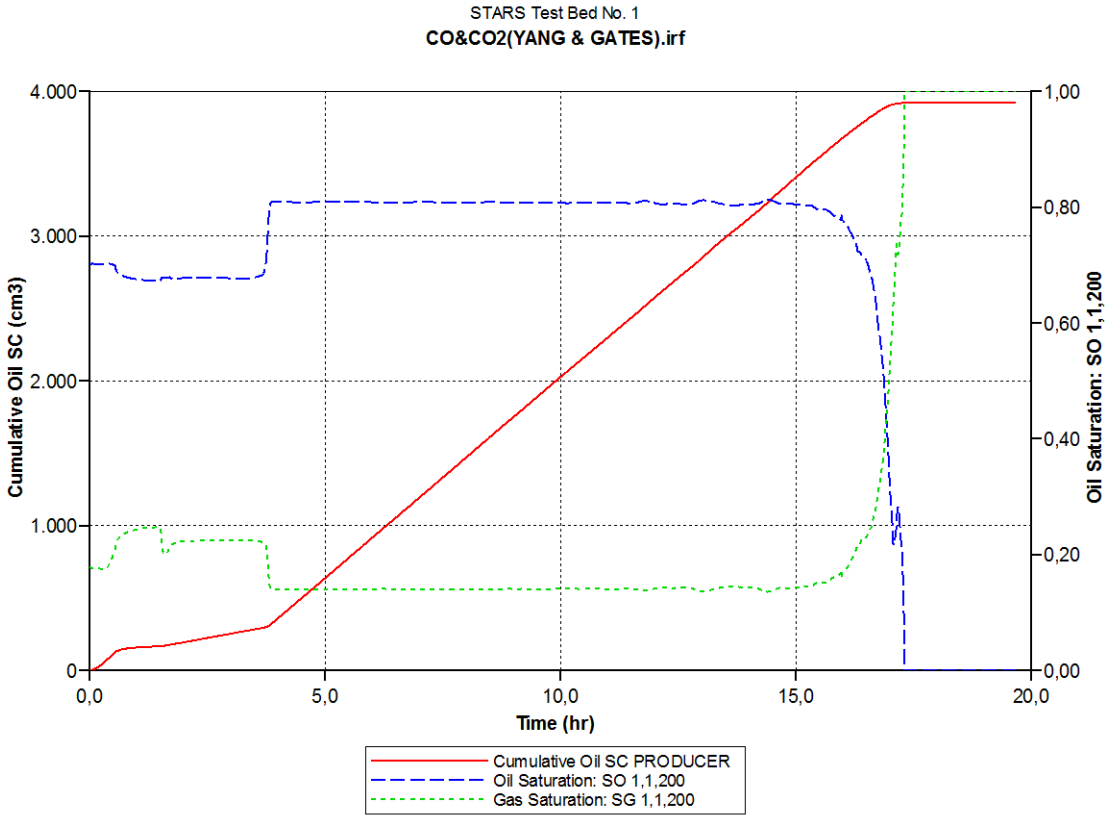

Figure 4.1. 4: Oil and gas saturation and cumulative oil production at the producer (1,1,200) as function of time; base case simulation.

In figure 4.1.4 the gas and oil saturation and the cumulative oil production at the producer are shown. It is interesting to note that the oil saturation drops after one hour. This coincides with the stagnation of the oil production while the gas saturation rises. This is an indication that the initial oil production is due to gas drive. The gas drive is due to evaporation of the lighter components of the oil and not due to CO_2 and CO formed by combustion (see Figure 4.1.5). In Figure 4.1.5 it can be seen that the main production of CO_2 and CO is from coke combustion; gas phase combustion hardly takes place. Only in the first few hours (2 hours) methane combustion takes place (see Figure 4.1.5). However, the amount of the produced CO_2 and CO is so small that it cannot explain the increase in gas saturation as it is observed (see Figure 4.1.4). The production of CO and CO_2 from CH_4 stops after 2 hours because all CH_4 initially present in the reservoir has been used and there is no further CH_4 produced. The production of CO and CO_2 from hydrocarbon gases is very low. However, analyzing the results it can be seen that anyhow the production of hydrocarbon gases from asphaltenes is very limited (see also Figure 4.1.5, 4.1.6 and Figure 3.3). In Figure 3.3 it can be seen that reaction #3 (production of hydrocarbon gas from asphaltenes) is the third slowest reaction at temperature below 350 °C but the second fastest reaction at temperatures above 500 °C. Because the oil saturation is zero at temperatures above 500 °C (see Figure 4.1.4), only a small quantity of hydrocarbon gas is formed by asphaltenes (see Figure 4.1.5 and 4.1.6).

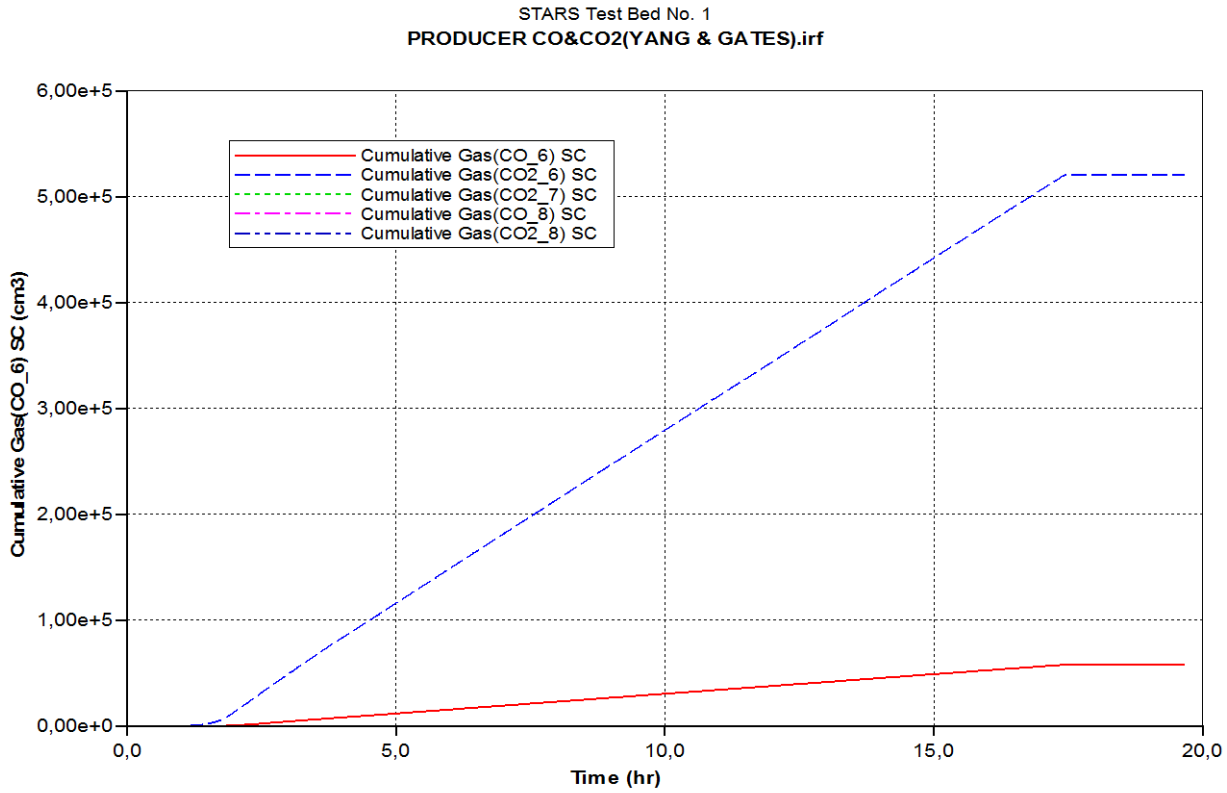

Figure 4.1. 5: Cumulative production of CO and CO_2 as function of time. The CO_2 and CO are split up according to their sources; base case simulation.

In figure 4.1.5 it can be seen that no CO_2 and CO formed by coke combustion is produced after about 18 hours. This indicates that the combustion front has moved through the combustion tube and no more coke is present in the combustion tube after 18 hours (see figure 4.1.7).

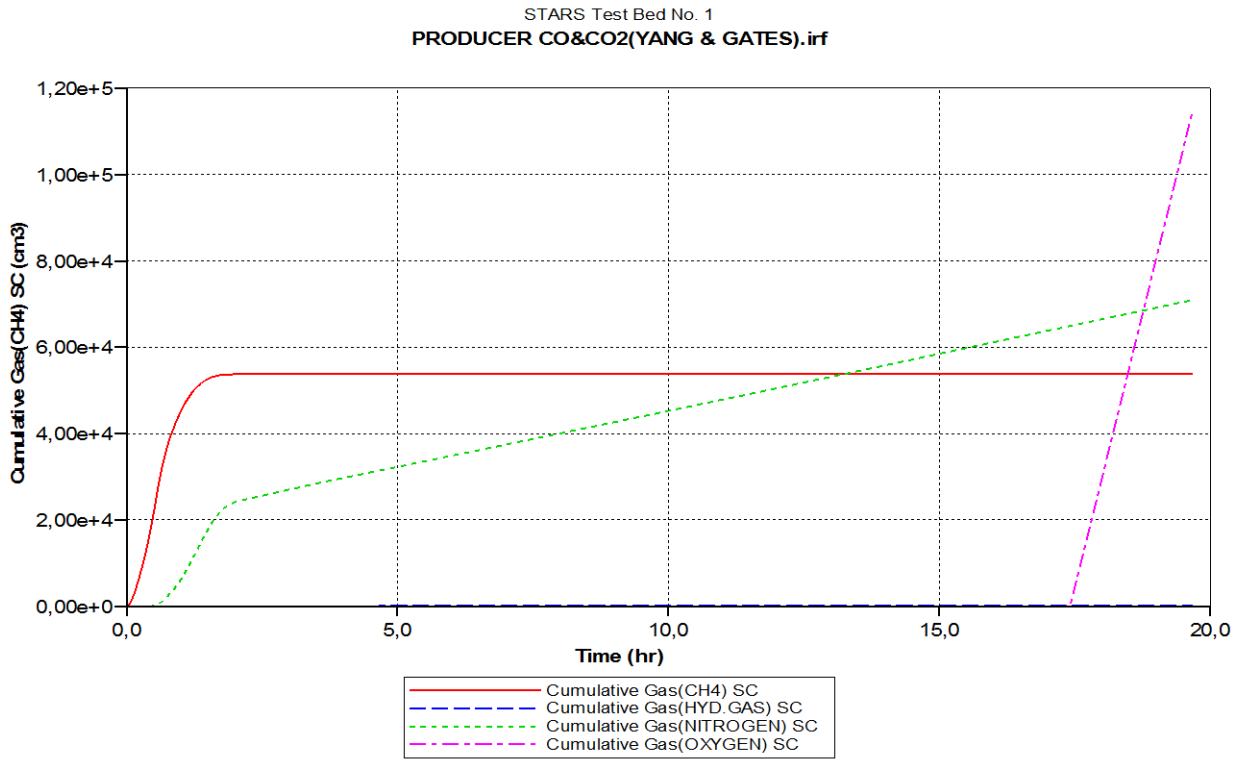

Figure 4.1. 6: Cumulative production curve of CH_4, HC gas, nitrogen and oxygen; base case simulation.

In figure 4.1.6 the gas phase composition of the produced gas is shown. It can be seen that after about 18 hours oxygen breakthrough occurs which coincides with the stop of the oil production. This shows that the oil production is indeed a combination of gas drive and combustion.

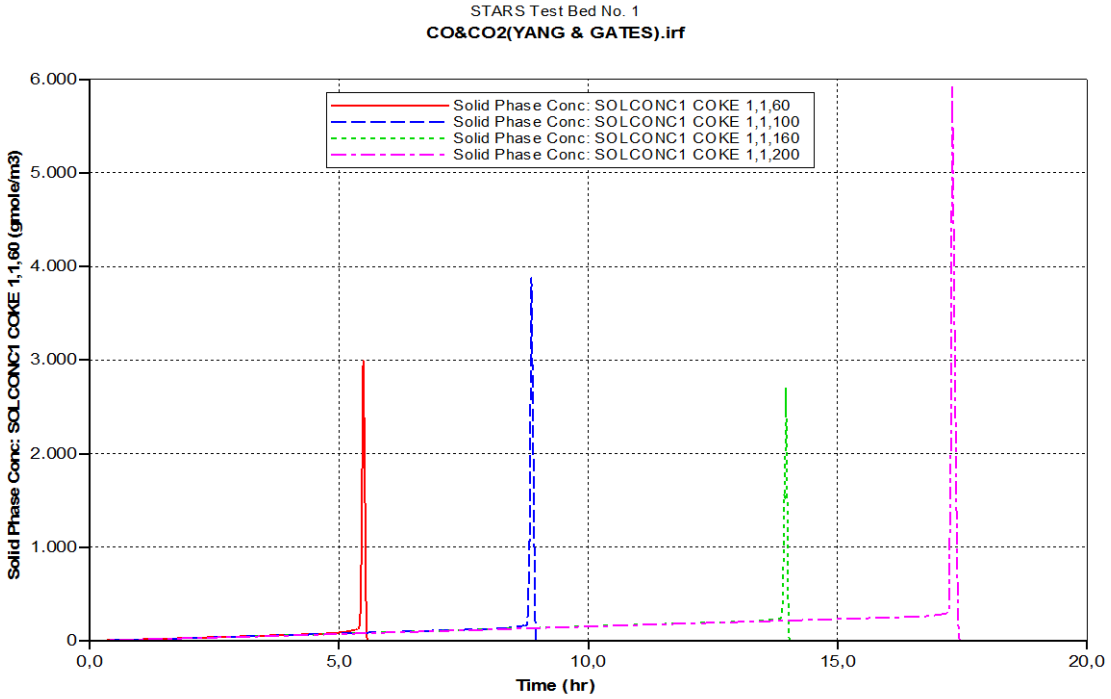

Figure 4.1. 7: The coke concentration profiles ($gmole/m^3$) at (1,1,60), (1,1,100), (1,1,160) and (1,1,200); base case simulation.

In figure 4.1.7 the coke concentration profiles ($gmole/m^3$) is visible. The figure shows that after 18 hours no more coke is present in the reservoir.

HC Gas combustion		
Cum. Oil Production	3918	cm^3
Cum. Gas Production	818741	cm^3

Table 4.2. 1: Cumulative oil and gas production; simulation #2

Introduction to simulation

In the base case of the simulations it was assumed that the methane gas phase combustion reaction is much slower than the hydrocarbon gas phase combustion (see Figure 3.2 and 3.3). This is an odd choice by Yang & Gates (2009) because essentially both are hydrocarbon gas combusting reactions. In this study the description of the reaction kinetics for the methane combustion was set equal to that of hydrocarbon gas phase combustion. This simulation will be called simulation #2 in the analysis and discussion below.

Summary

In the base case no hydrocarbon gas combustion takes place (see Figure 4.1.5). In this simulation 185 cm^3 (sc) CO_2 and 180 cm^3 (sc) CO is produced by reaction #8. This is insignificant compared to the total CO & CO_2 production of roughly 600 000 cm^3 (see figure 4.2.3). The total hydrocarbon gas production is insignificant compared to the CH_4 production (see figure 4.2.4). The cumulative oil and gas production and temperature profiles were not significantly different from the base case (see Figure 4.2.1). Overall, there are no significant changes in the results compared to the base case.

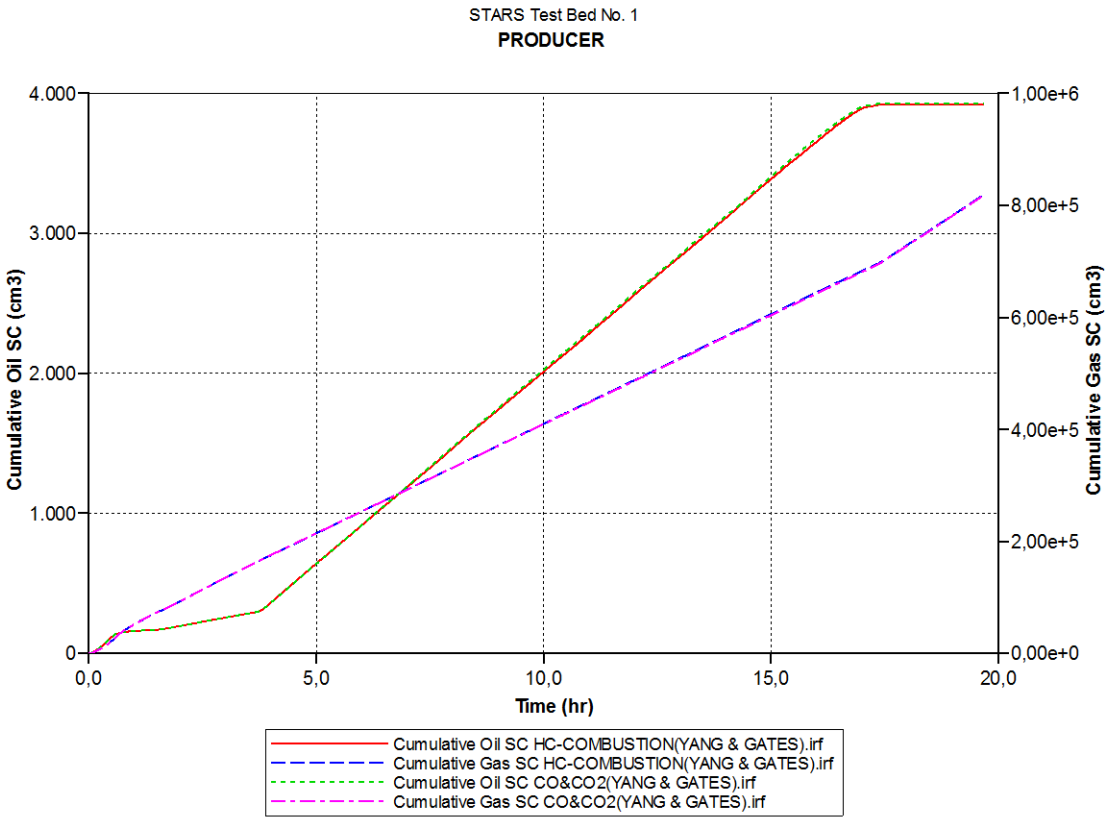

Figure 4.2. 1: The cumulative oil and gas production; base case and simulation #2.

Figure 4.2.1 shows the cumulative oil and gas production from the base case and simulation #2. The graphs from the two simulations do not differ from each other.

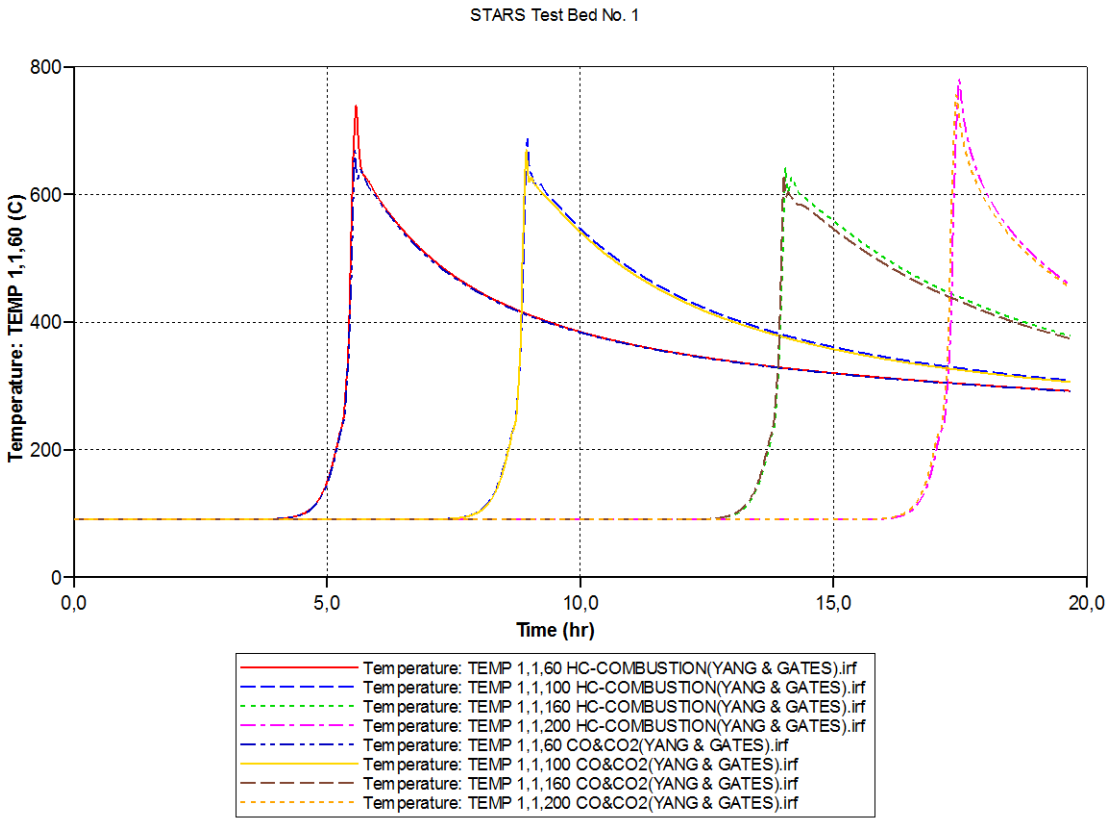

Figure 4.2. 2: This figure shows the temperature profile at (1,1,60), (1,1,100), (1,1,160) and (1,1,200); base case simulation and simulation #2.

Figure 4.2.2 shows the temperature graphs at various positions for the base case simulation and simulation #2. The graphs from the two simulations do not differ from each other significantly.

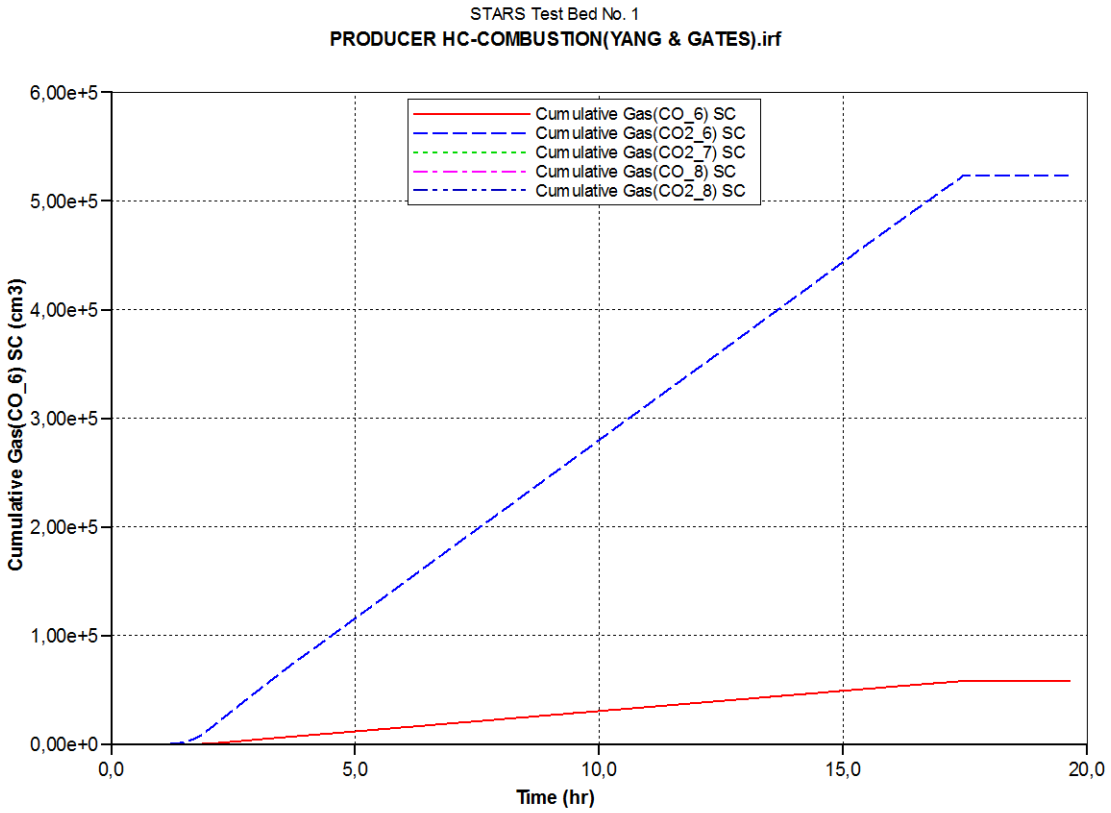

Figure 4.2. 3: Cumulative production of CO and CO_2 formed by the combustion reactions; simulation #2

Figure 4.2.3 shows the cumulative production of CO_2 and CO formed by the combustion reactions. It can be seen that the CO and CO_2 formed by the combustion of hydrocarbon gas and methane are insignificant compared to coke combustion.

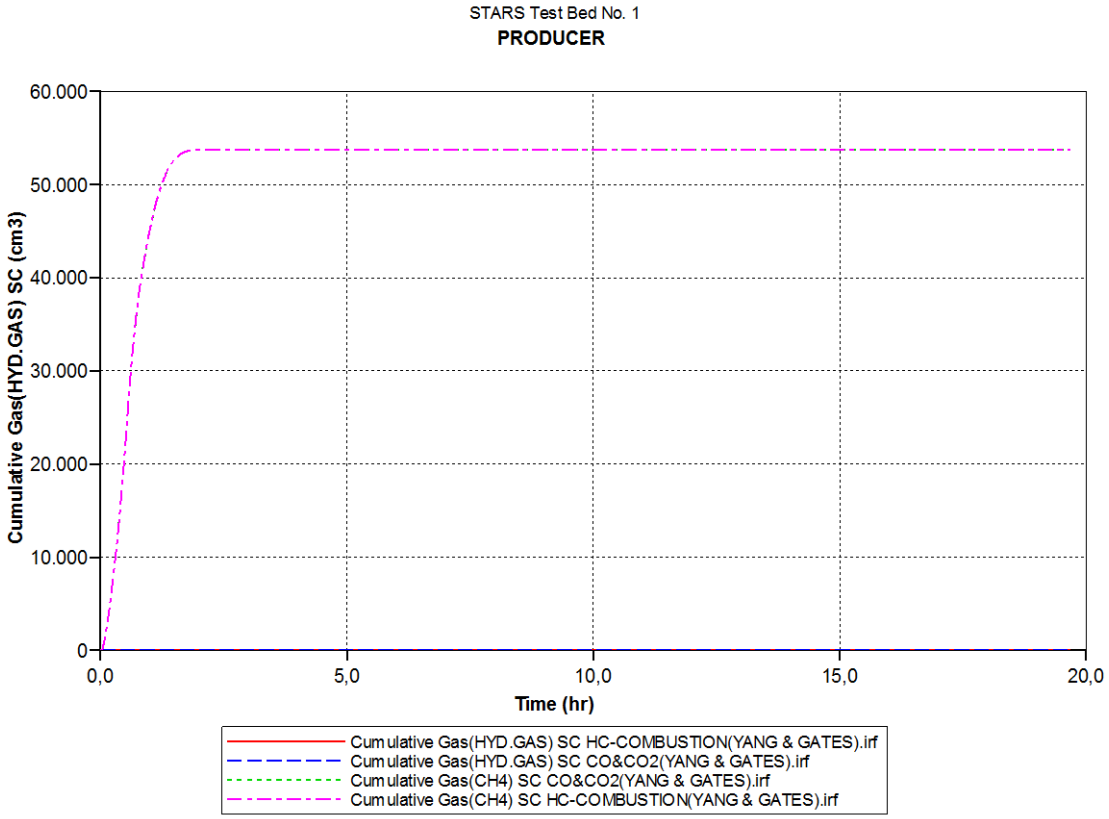

Figure 4.2. 4: The cumulative gas production of hydrocarbon gas and methane; base case simulation and simulation #2.

Figure 4.2.3 shows the cumulative production of hydrocarbon gas and methane from the base case simulation and simulation #2. The hydrocarbon gas production curves from the two simulations do not differ from each other. It can also be seen that the total hydrocarbon gas production (about 20 cm^3 in the base case and about 90 cm^3 in simulation #2) is insignificant when compared to the methane production.

Reaction #2 & #5 switched		
Cum. Oil Production	3265	cm^3
Cum. Gas Production	874284	cm^3

Table 4.3. 1: total oil and gas produced

Total effluent HC Gas	
Base Case	90 cm^3
Reaction kinetics reactions #2 and #5 switched	490 cm^3

Table 4.3. 2: total effluent hydrocarbon gas

Introduction to simulation

Yang & Gates (2009) assumed that the reaction rate of reaction #2 is higher than that of reaction #5 (see Figure 3.3). According to Yang & Gates (2009) reaction #2, a cracking reaction, starts to produce coke at a temperature of 90 °C. Reaction #5, a Low Temperature Oxidation (LTO) reaction, starts to produce coke at a temperature of 400 °C[5]. From experimental data it can be seen that cracking does not occur at these temperatures[11] and according to its definition an LTO reaction does not occur at temperatures above 350 °C[6]. This simulation is initiated with the reaction kinetics of reaction #2 and #5 switched to evaluate their influence on their simulation. This simulation with the reaction kinetics of reactions #2 and #5 switched (see table 3.3) is called simulation #3 in the analysis and discussion below.

Summary

In simulation #3 more cumulative gas is produced than in the base case (see Table 4.3.1 and 4.1.1), this is due to an increase in coke formation and its combustion (see Figure 4.3.6). Less cumulative oil is produced than in the base case (see Table 4.3.1 and Figure 4.3.1). This is because more oil is formed into coke than in the base case (see Figure 4.3.4). Unlike in the base case, oxygen breakthrough never occurs (see Figure 4.3.7), which indicates a possible oxygen shortage. In table 4.3.2 it can be seen that more hydrocarbon gas is produced in this simulation than in the base case which is due to the combustion front moving slower through the combustion tube than in the base case, giving more time for hydrocarbon gas to be formed.

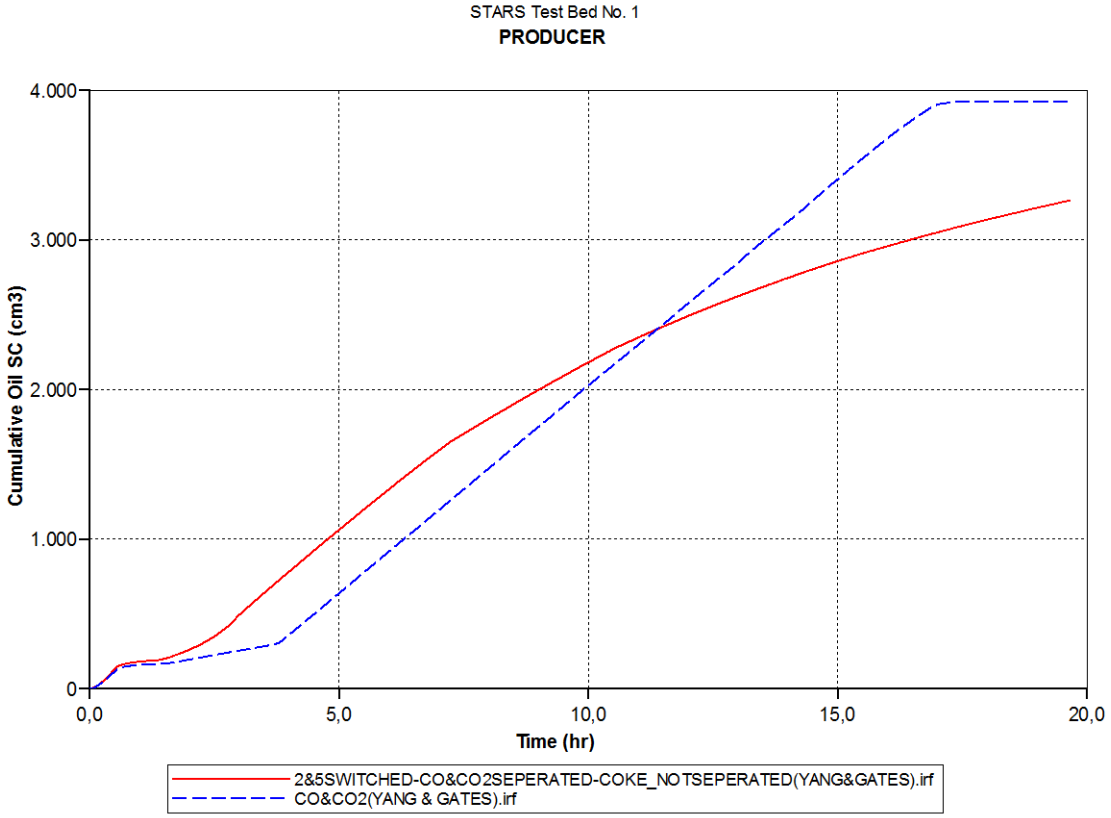

Figure 4.3. 1: The cumulative production of oil at standard conditions; base case simulation and simulation #3.

Figure 4.3.1 shows that cumulative production of oil in the base simulation and simulation #3. It can be seen that in both simulations the oil production stagnates after one hour. The oil production in simulation #3 continuous about two hours later but slows down over time. Unlike in the base case simulation, the oil production does not stop after 18 hours (or 20 hours) in simulation #3.

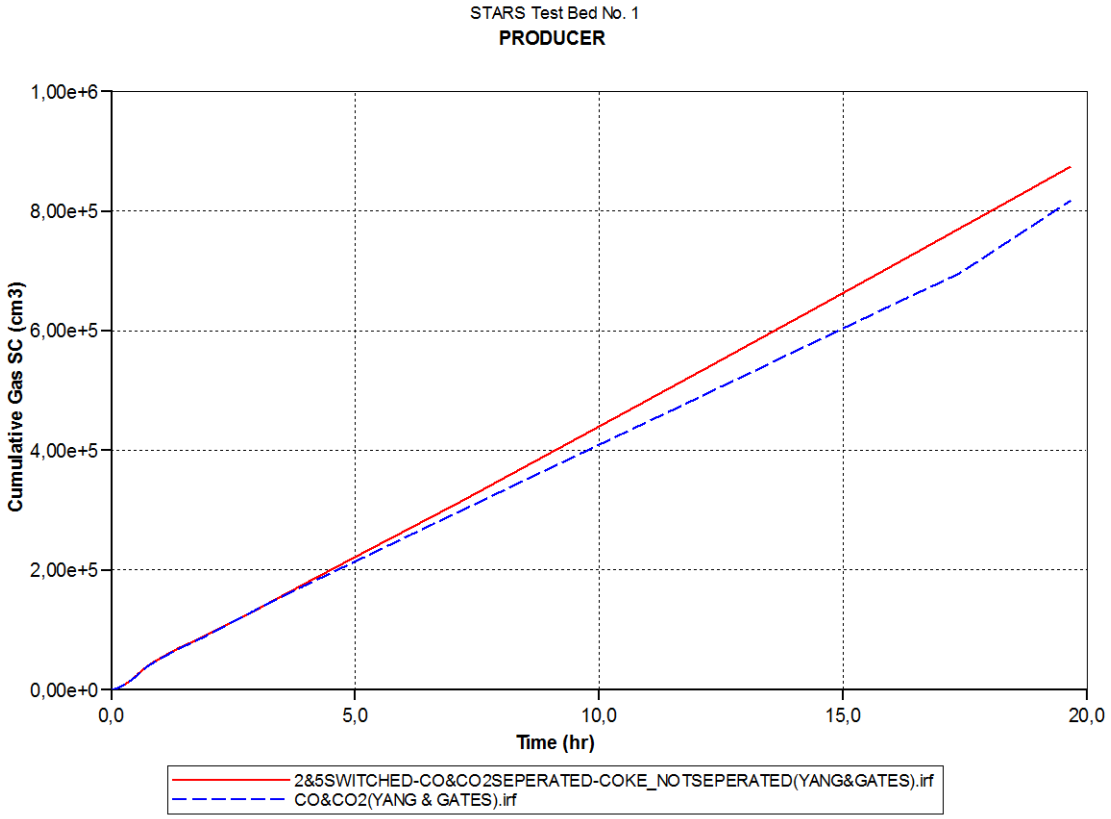

Figure 4.3. 2: Cumulative gas production at standard conditions; base case simulation and simulation #3.

Figure 4.3.2 shows the cumulative gas production in the base case simulation and simulation #3. Because the cumulative gas production curve is steeper for simulation #3 than in the base case, it can be concluded that the gas production is higher in simulation #3 than in the base case. Furthermore, unlike in the base case the gas production does not change after 18 hours, which indicates that the combustion front does not move through the combustion tube in 20 hours.

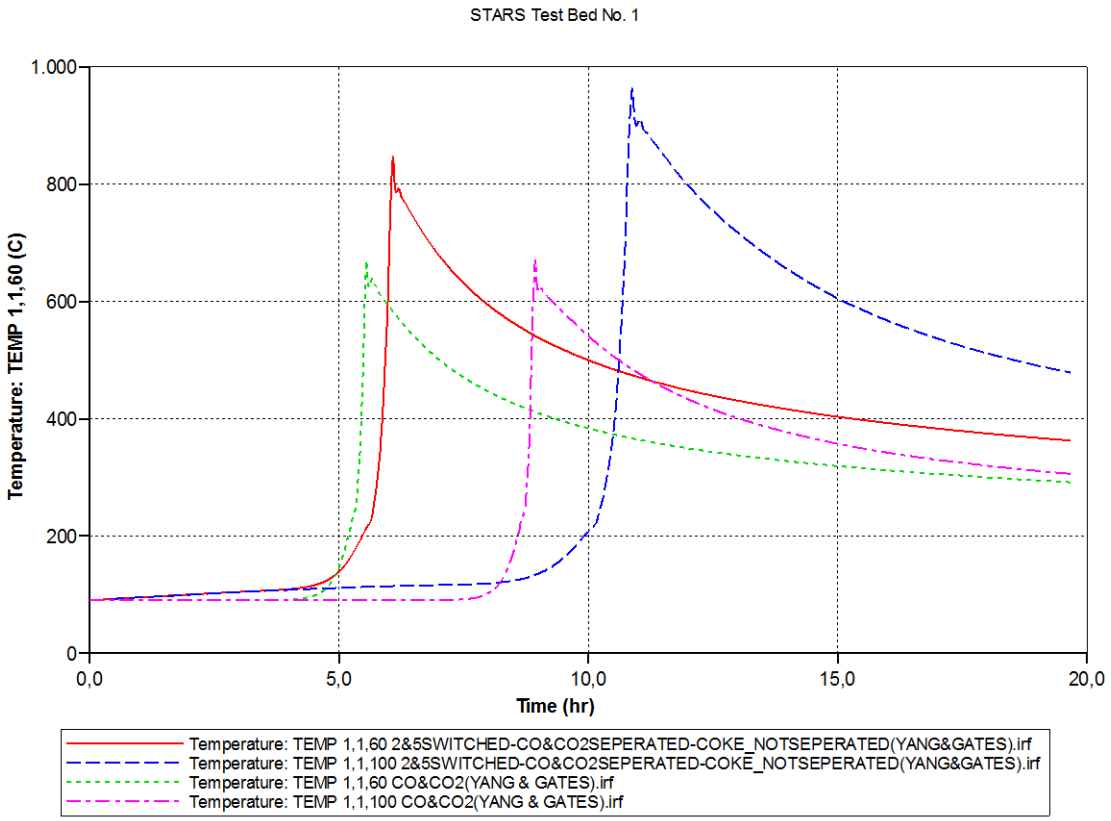

Figure 4.3. 3: The temperature profiles at (1,1,60) and (1,1,100); base case simulation and simulation #3.

Figure 4.3.3 show the temperature profiles at (1,1,60) and (1,1,100) for the base case simulation and simulation #3. The temperature profiles show that higher temperatures are achieved in simulation #3 than in the base case, which indicates that more coke is produced than in the base case. Unlike in the base case, the temperatures at (1,1,60) and (1,1,100) in simulation #3 already start to rise from the beginning. This indicates that coke is formed and combusted from the beginning.

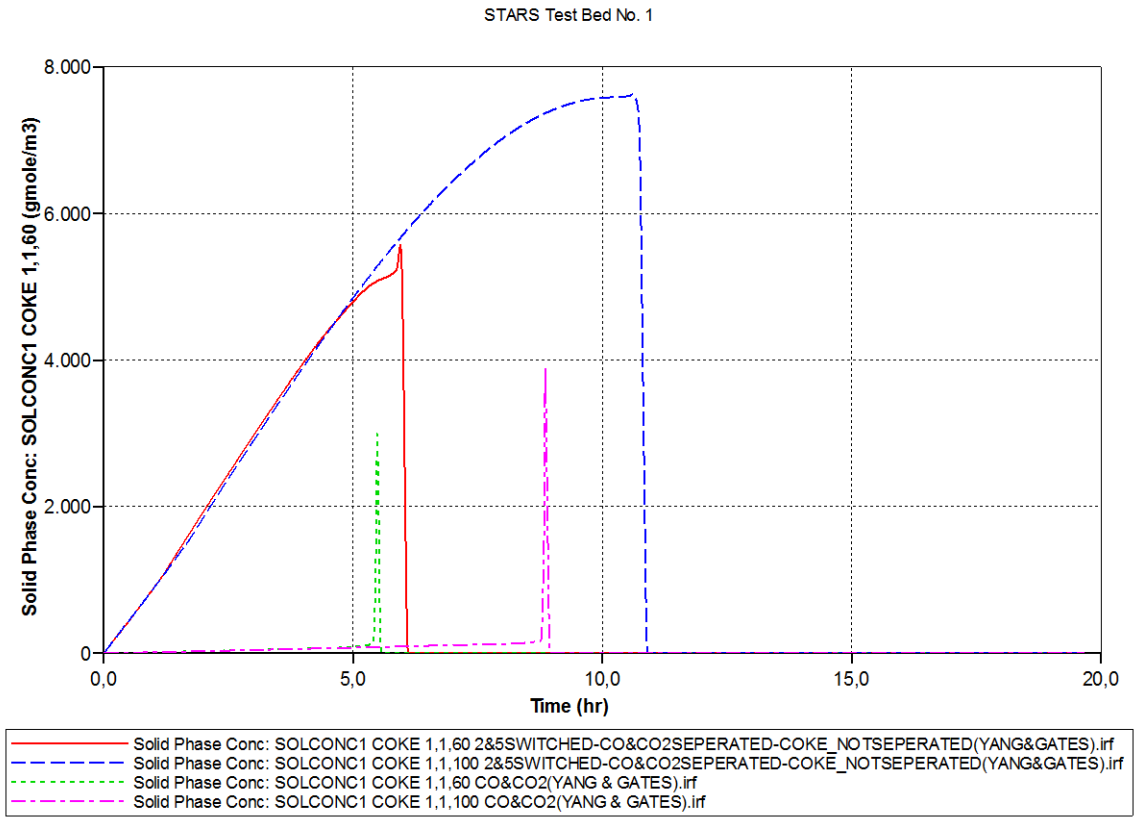

Figure 4.3. 4: Coke concentration ($gmole/m^3$) at (1,1,60) and (1,1,100); base case simulation and simulation #3.

Figure 4.3.4 shows the coke concentration at (1,1,60) and (1,1,100) for the base case simulation and simulation #3. It can be seen that the coke concentration start to rise from the beginning at (1,1,60) and (1,1,100) at the same rate in simulation #3. This means that as the combustion front moves through the combustion tube, it will encounter more coke to combust and less oil to displace. Which could be the reason why oil production slows down over time in simulation #3 (see Figure 4.3.1). It can also be seen that the coke concentration drops to zero (and thus the coke combustion) earlier in the base case simulation than in simulation #3 at coinciding positions. Which could mean that the combustion front does not move through the combustion tube in 20 hours, which is why the oil production does not stop in simulation #3 (see Figure 4.3.1).

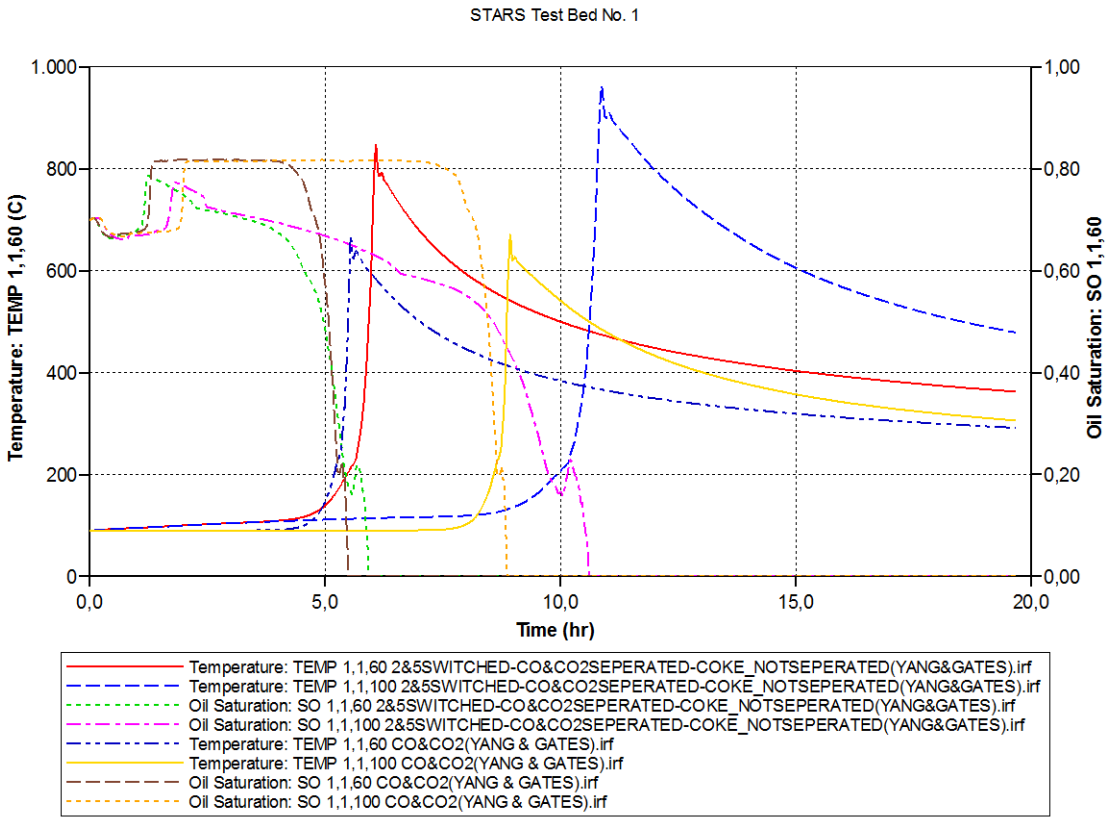

Figure 4.3. 5: The oil saturation at (1,1,60) and (1,1,100); base case simulation and simulation #3.

Figure 4.3.5 shows the oil saturation at (1,1,60) and (1,1,100) for the base case simulation and simulation #3. It is visible that in simulation #3 the oil saturation starts to decline at (1,1,60) and (1,1,100) before the combustion front has reached those positions. This indicates that the combustion front displaces less oil as it moves through the combustion tube, explaining why the oil production rate slows down over time (see Figure 4.3.1).

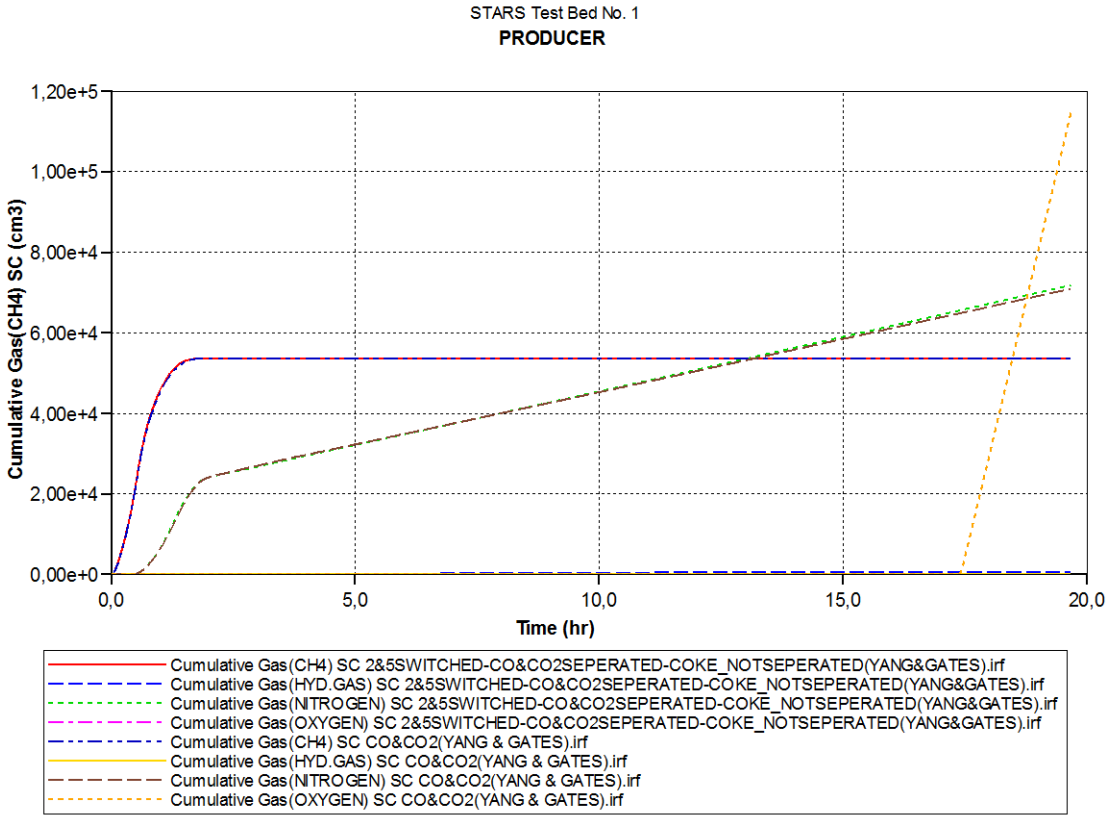

Figure 4.3. 6: The cumulative production of the different gasses; simulation #3

Figure 4.3.5 shows the cumulative production of the different gasses in simulation #3. It shows that no oxygen breakthrough occurs, which is why the cumulative gas production does not change after 18 hours (see Figure 4.3.2). This also indicates that the combustion front has not moved through the combustion tube by the end of the simulation. A bit more hydrocarbon gas is produced than in the base case due to the combustion front moving slower through the combustion tube, giving more time for reaction #3 to form hydrocarbon gas from asphaltenes before it is displaced by the combustion front

Higher/lower injection flow rate

Lower injection rate production data in cm^3				
	Base case	Lower injection rate	Difference	Percentage
Asphaltene	721.8	483.06	-238.74	-33.08%
Maltene	3203.04	2097.82	-1105.22	-34.51%
Total oil	3924.8	483.06	-3441.74	-87.69%
HC Gas	86.49	209.93	123.44	142.72%
CO_2 by HTO	520472	314924	-205548	-39.49%

Table 4.4. 1: Production data with an injection rate of 0.75 m^3/day.

Higher injection rate production data in cm3				
	Base case	Lower injection rate	Difference	Percentage
Asphaltene	721.8	725.5	3.7	0.51%
Maltene	3203.04	3228.3	25.26	0.79%
Total oil	3924.8	3953.8	29	0.74%
HC Gas	86.49	12.88	-73.61	-85.11%
CO2 by HTO	520472	551895	31423	6.04%

Table 4.4. 2: Production data with an injection rate of 2.00 m^3/day.

Introduction to this simulation

In the base case the oxygen production starts after 18 hours (see Figure 4.1.6). This indicates a possible oxygen shortage in the simulation in the first 18 hours. In literature it is stated that the fuel/oxygen ratio is crucial for the success of in-situ combustion The shortage is possibly causing the oxygen consuming reactions not taking place at their full speed or not taking place altogether. Increasing the air injection rate significantly (from 1.334 m^3/day to 2 m^3/day) can possibly cause some reactions to take place faster. A second simulation is made with a lower air injection rate (0.75 m^3/day) to check if correct conclusions are made. The simulation with a higher injection rate and lower injection rate are called simulation #4 and #5 respectively in the analysis and discussion below.

Summary

Increasing the injection rate results in a slight increase of the oil and gas production (table 4.4.1 and 4.4.2). More asphaltenes, maltenes and coke are produced, yet less hydrocarbon gas is produced. The temperatures achieved are higher than in the base case with an increased injection rate. These results are the opposite if the injection rate is reduced.

Analysis

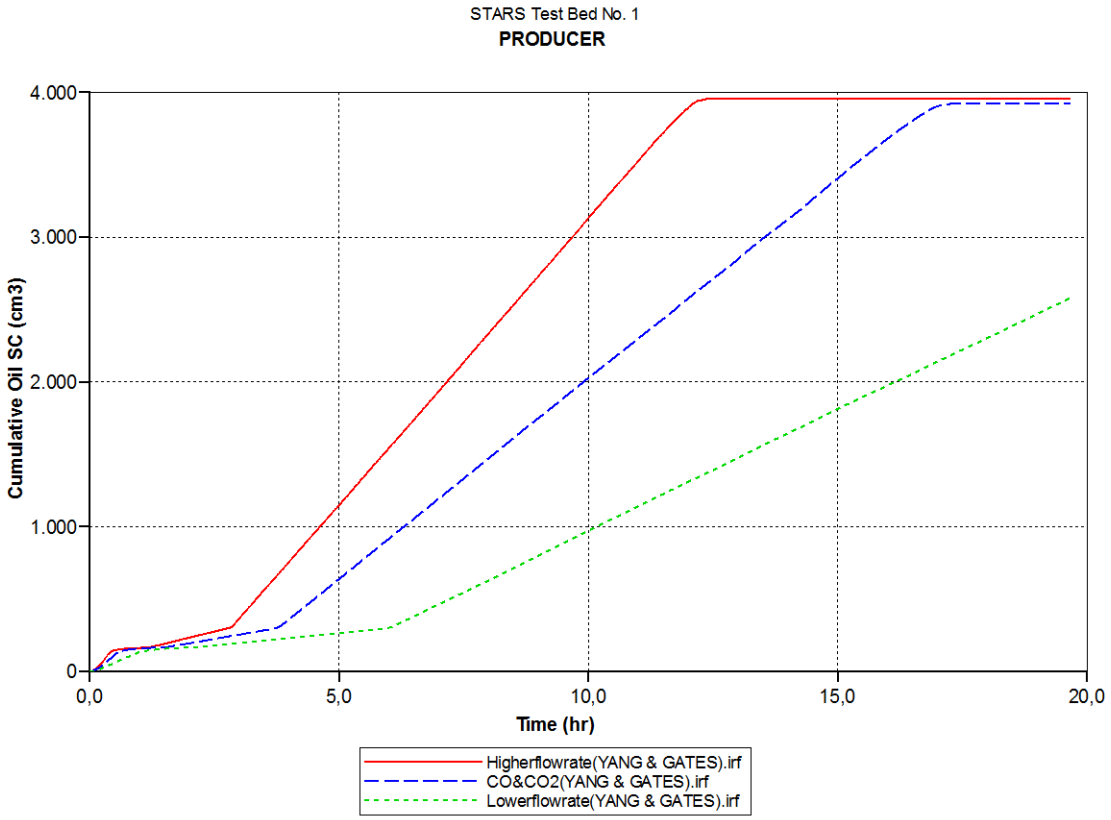

Figure 4.4. 1: The cumulative oil production; base case, simulation #4 and #5.

Figure 4.4.1 shows the cumulative oil production for the base case and simulation #4 and #5. It can be seen that a bit more oil is produced with a higher injection rate. Lowering the injection rate causes the oil production to decrease significantly. It is also visible that with a higher injection rate the oil production stops sooner than in the base case, indicating that the combustion front moves faster through the reservoir. This could be due to higher oxygen availability than in the base case, leading more hydrocarbons to be oxidized per time unit, causing the combustion front to move faster.

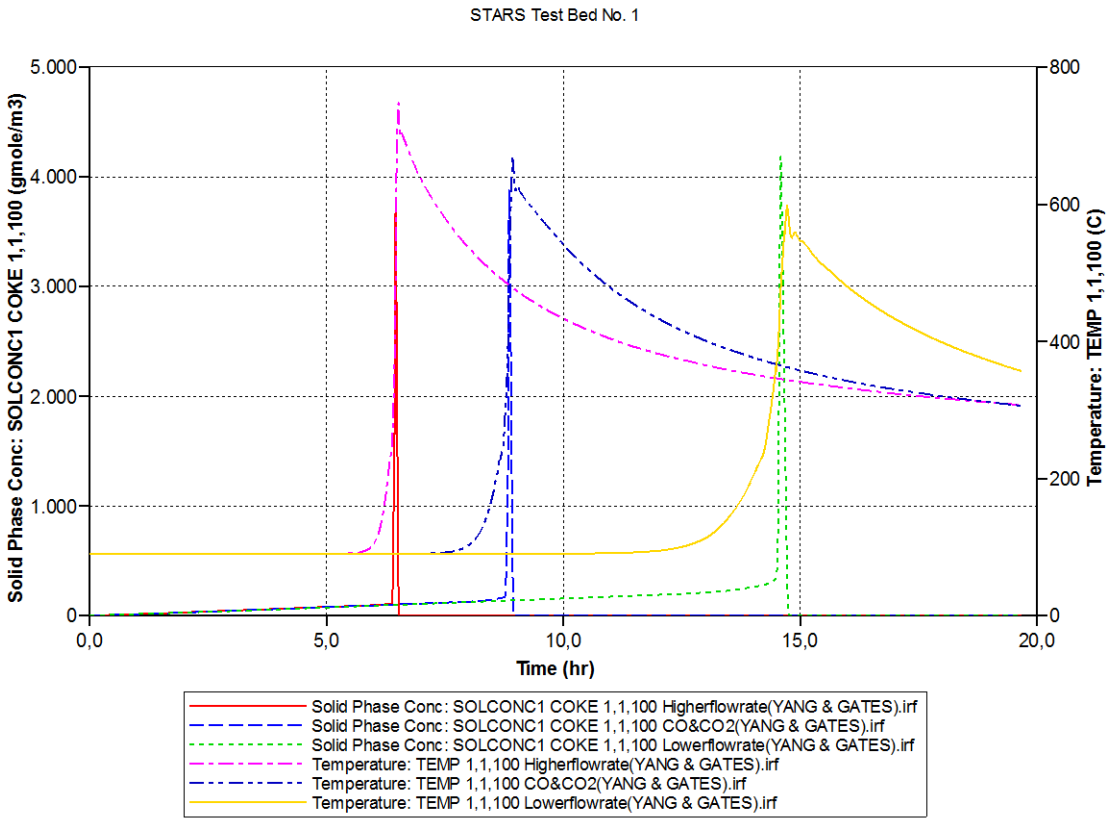

Figure 4.4. 2: The temperature and coke concentration graphs at (1,1,100); base case and simulation #4 and #5.

Figure 4.4.2 shows the temperature and coke concentrations at (1,1,100), the middle of the combustion tube, for the base case and simulation #4 and #5. It can be seen that with a higher injection rate the combustion front moves faster through the reservoir. The coke concentration profile is about the same for all three simulations, indicating that the cracking reaction (which produces the coke in the beginning[5]) is not affected by the variation of the injection rate. A higher temperature is achieved with a higher injection rate than in the base. It is also visible that the temperature rises steeper than in the base case, which indicates that probably more coke is combusted per time unit than in the base.

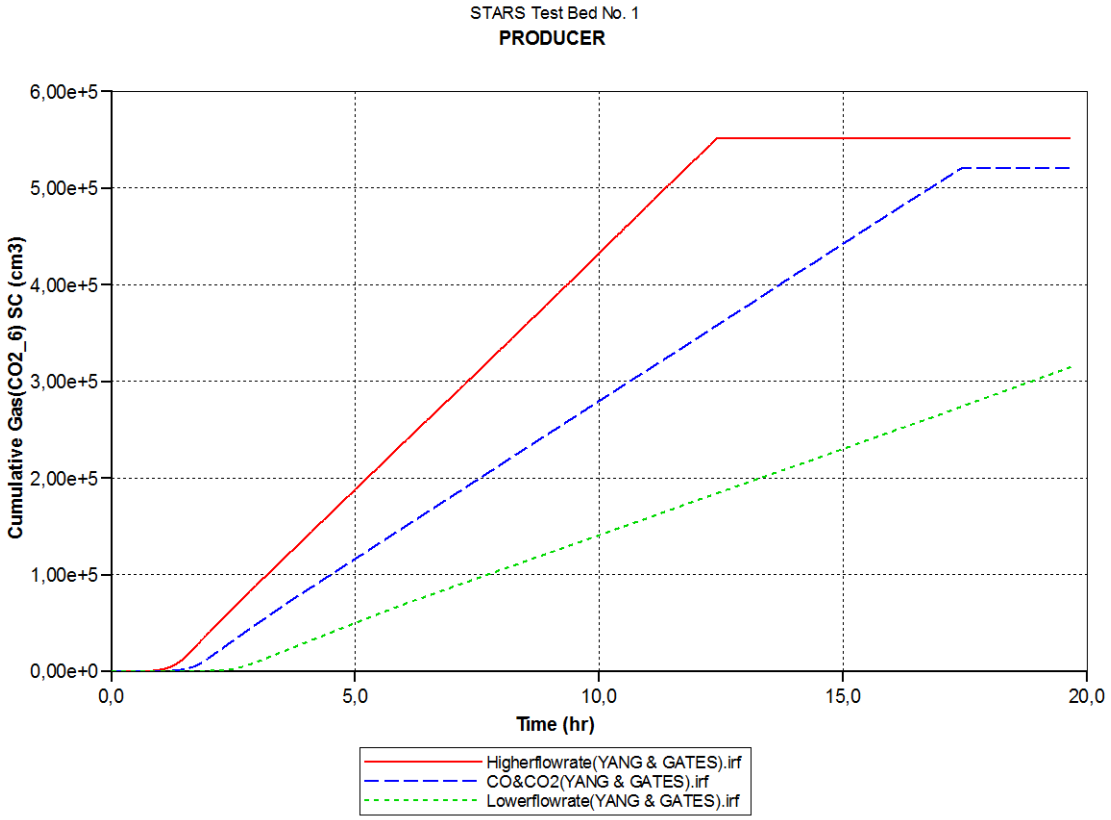

Figure 4.4. 3: The cumulative produced CO_2 which is formed by coke combustion (HTO); Base case and simulation #4 and #5

Figure 4.4.3 shows the cumulative produced CO_2 which is formed by coke combustion (chemical reaction #6). It is shown that more CO_2 formed by HTO is produced with a higher injection rate. Which indicate that more coke is formed with a higher injection rate than in the base case. Figure 4.4.2 shows that the maximum coke concentration is lower with an increased injection rate. This indicates that the coke combustion rate is higher than in the base case, which is due to abundance in oxygen. With a higher injection rate, reaction #5 takes place faster because oxygen is widely available; this is probably the reason for more coke formation with a higher injection rate.

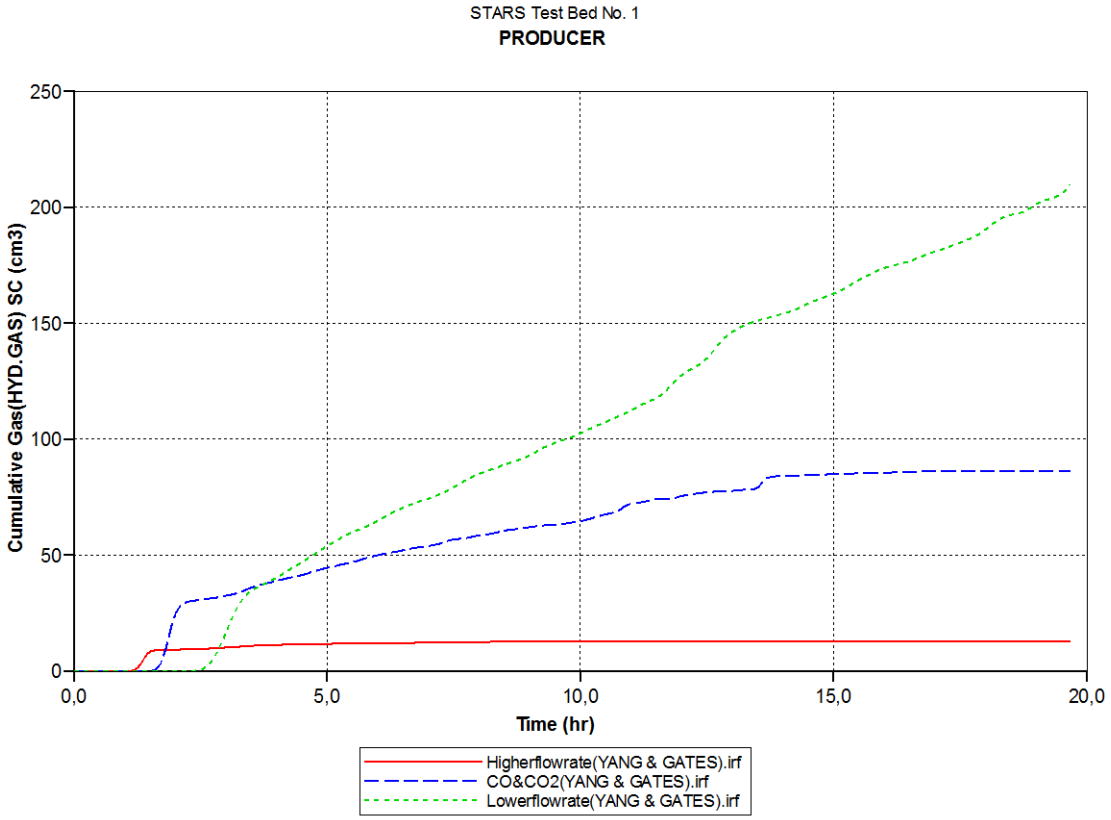

Figure 4.4. 4: The cumulative produced hydrocarbon gas; base case simulation and simulation #4 and #5.

Figure 4.4.4 shows the cumulative produced hydrocarbon gas for the base case simulation and simulation #4 and #5. It is clearly visible that less hydrocarbon gas is produced with a higher injection rate. With a higher injection rate, the combustion front moves through the reservoir faster, giving less time for reaction #3 to form hydrocarbon gas. This is probably the reason why more oil is produced with a higher injection rate than in the base case.

Conclusions

Influence of the hydrocarbon gas combustion reaction

In the base case of the simulations it was assumed that the methane gas phase combustion reaction is much slower than the hydrocarbon gas phase combustion. In this study the description of the reaction kinetics for the methane combustion and the hydrocarbon gas phase combustion were described in the same manner. From the results it can be seen that there is hardly any effect on the cumulative oil and gas production or the temperature profile. The changes are less than 3% vol. compared to the base case (see table 4.2.1 and figures 4.2.1 to 4.2.4). From this can be concluded that this change has no significant effect on the coke formation. However, this might be also caused by the fact that in general the effect of gas phase combustions is estimated which is then reflected in choice of reaction parameters. If experiments show that gas phase combustion has no effect on the overall process, these reactions should excluded from the reaction schemes.

Coke formation from asphaltenes

This simulation is initiated with the reaction kinetics of reaction #2 and #5 (see table 3.3) switched to evaluate their influence on their simulation. As a result about 25% vol. less oil is produced than in the base case and about 8% vol. more gas (see also table 4.3.1and figures 4.3.1 and 4.3.2). Further, more coke is produced and combusted than in the base case, which can be seen from the total CO_2 produced by the HTO reaction (see fig. 4.3.4). These are significant changes to the outcome of the simulation compared to the base case.

The outcome shows that the reaction kinetics of reaction #2 and #5 have a strong influence on the simulation results. It is therefore of great importance to understand these reactions thoroughly to build an ISC simulation model. It is advised to investigate these reactions to better understand their reaction kinetics.

Higher/lower flow rate of injected air

In literature it is stated that the fuel/oxygen ratio is crucial for the success of in-situ combustion[12]. A higher air injection rate means that more oxygen is available for combustion. This can be seen in the higher oil production and coke formation. At the same time the maximum temperatures reached in the combustion tube have increased which further support that also more coke is combusted. Due to the higher air injection rate the combustion front moves faster through the reservoir than in the base case (see also table 4.4.1and 4.4.2 and figures 4.4.1 to 4.4.5). This means that it is possibly economically more favorable to inject air at a higher rate into an oil reservoir in which ISC is conducted.

In practice, one of the easiest parameters to vary when applying In-Situ Combustion as an EOR method is the injection rate of the air. The results show that it is possibly favorable economically to raise the injection rate of the air due to a higher velocity of the fire front and higher oil recovery. Therefore it is advised to do a tube combustion experiment with a raised injection rate of the air to also investigate if at a higher injection rate oxygen break-through also occurs earlier.

Combined conclusion

This research shows that the fastest reactions are not always the dominant reactions which is visible in the simulation where hydrocarbon gas was defined as the fastest reaction. Increasing the injection rate of the air can have a small effect on the results while reducing the injection rate can have a major effect on the results, which shows that not all reactions have the same significance. Defining the input parameters for the two coke forming reactions in a clearly wrong chemical-physically[4, 11], delivers results which coincide with experiment data[5]. This research shows that chemical reactions which are defined in the simulator should be understood thoroughly and that making a good ISC simulator is not merely fitting input parameters to production data.

References

[1] http://www.cfr.org/netherlands/royal-dutch-shell-ceo-end-easy-oil/p15923
[2] Moore, Belgrave, Mehta, Ursenbach, Laurenshen, Xi (1992)
[3] Akin, Kok, Bagci (2000)
[4] Aske et al. (2002)
[5] Yang & Gates, 2006
[6] Marin, 2007
[7] Gluyas & Swarbrick (2004)
[8] Simmie (2003)
[9] Belgrave et al. (1990)
[10] http://www.cmgroup.com/software/stars.htm
[11] Hayashitani et al., 1987
[12] Hensel, James, Gordon (1984)